

Technical University of Denmark



## Multigroup cross sections for reactor physics calculations generated on the basis of fundamental nuclear data

Larsen, Anne Margrethe Hvidtfeldt

*Publication date:*  
1973

*Document Version*  
Publisher's PDF, also known as Version of record

[Link back to DTU Orbit](#)

*Citation (APA):*

Hvidtfeldt Larsen, A. M. (1973). Multigroup cross sections for reactor physics calculations generated on the basis of fundamental nuclear data. (Denmark. Forskningscenter Risoe. Risoe-R; No. 286).

## DTU Library

Technical Information Center of Denmark

---

### General rights

Copyright and moral rights for the publications made accessible in the public portal are retained by the authors and/or other copyright owners and it is a condition of accessing publications that users recognise and abide by the legal requirements associated with these rights.

- Users may download and print one copy of any publication from the public portal for the purpose of private study or research.
- You may not further distribute the material or use it for any profit-making activity or commercial gain
- You may freely distribute the URL identifying the publication in the public portal

If you believe that this document breaches copyright please contact us providing details, and we will remove access to the work immediately and investigate your claim.

Danish Atomic Energy Commission  
Research Establishment Risø

---

# Multigroup Cross Sections for Reactor Physics Calculations, Generated on the Basis of Fundamental Nuclear Data

by A. M. Hvidtfeldt Larsen

March 1973

*Sales distributors:* Jul. Gjellerup, 87, Sølvgade, DK-1307 Copenhagen K, Denmark

*Available on exchange from:* Library, Danish Atomic Energy Commission, Risø, DK-4000 Roskilde, Denmark

Multigroup Cross Sections for Reactor Physics  
Calculations, Generated on the Basis of Fundamental  
Nuclear Data

by

A. M. Hvidtfeldt Larsen

Danish Atomic Energy Commission

Research Establishment Risø

Reactor Physics Department

Abstract

The set-up of a cross section generating code system based on fundamental nuclear data is described. The basic source of data is the UK Nuclear Data Library containing cross section tabulations for most of the materials important in Reactor Physics Calculations. Effective resonance cross sections calculated from resonance parameters are added together with thermal scattering data. The applicability to light-water reactor systems of the group cross sections produced is demonstrated by means of calculationally simple test examples.

CONTENTS

	Page
1. Introduction .....	5
2. Principles for the Data System Set-up .....	5
3. Data System Description .....	8
3.1. The SIGMA MASTER TAPE .....	9
3.2. Resonance Treatment .....	9
3.3. Thermal Scattering .....	13
3.4. The CRS Program .....	14
3.5. Communication to the Reactor Physics Programs Using the Cross Section Data .....	15
4. Calculations on Homogeneous Critical Spheres .....	17
4.1. U <sup>235</sup> Spheres .....	18
4.2. Pu Spheres .....	20
4.3. Methods of Calculation .....	22
4.4. Results of Sphere Calculations .....	24
5. Unit Cell Burn-up Calculations for the Yankee Rowe Reactor ..	31
5.1. The Yankee Core and the EYC Project .....	32
5.2. Unit Cell Burn-up Calculations .....	36
5.3. Multiplication Factors .....	37
5.4. Isotopic Concentrations .....	39
6. Unit Cell Criticality Calculations .....	50
6.1. Description of Critical Lattices .....	50
6.2. Calculated Multiplication Factors .....	53
7. Conclusion .....	59
Acknowledgements .....	59
References .....	60



## 1. INTRODUCTION

Throughout the world much effort is devoted to collecting and evaluating measured data for neutron interaction with matter. The evaluated "best values" of data relevant to reactor physics calculations are edited as evaluated data libraries and made available to the users in the form of magnetic data tapes. The work described in this report was undertaken in order to utilize the knowledge stored on these tapes for reactor physics calculation purposes.

A program system has been constructed for the production of multi-group cross sections on the basis of the British evaluated nuclear data library, UKNDL<sup>1, 2)</sup>. The tabulated data of the UKNDL have been converted into the so-called MASTER TAPE<sup>3)</sup> containing 76-group cross sections for all materials found in the UKNDL. This tape will be the starting point until the cross sections from an updated version of the UKNDL are substituted. In the program CRS<sup>4)</sup> the problem-dependent data for thermalization and resonance reactions are supplied. Flux calculations and condensation are also performed in the CRS code, and the resulting group cross sections are edited in a form ready for use in various reactor physics codes.

Test calculations performed as an investigation of the applicability of the data system to light-water reactor calculations are included in the report. The calculations are: Criticality calculations for spherical benchmark experiments, burn-up calculations for the Yankee Rowe reactor, and calculations of the effective multiplication factor for critical uniform lattices.

## 2. PRINCIPLES FOR THE DATA SYSTEM SET-UP

A number of requirements exist of a data system providing cross section data for reactor physics calculations, the specific requirements being dependent upon the sort of calculation to be performed. In our case it has not yet been decided to what reactor the data will be applied; not even the reactor type is known. For that reason a data system involving fittings to special problems is not at issue, and the only thing feasible is to base the cross section generating on fundamental nuclear data.

The accuracy in predicting different reactor physical quantities of importance to, for instance, *safety analysis* and reactor economy studies is greatly dependent on the accuracy of the nuclear data involved. It is generally accepted that the uncertainties on calculated integral quantities

should not exceed

- + 1% on  $k_{eff}$
- + 10% on isotopic inventories during burn-up,
- + 10% on material worth, and
- + 20% on Doppler coefficients.

Uncertainties in the calculations arise of course not only because of the cross sections, but also because of approximations in the calculational methods. A 1% error in the multiplication factor for a limited reactor region will cause an error in the overall power distribution of roughly 10%, and an accuracy of 10% in the power distribution is about the highest obtainable in realistic cases with the present methods of calculation, on the assumption that the cross section values are exactly known. So the 1 per cent accuracy demand on  $k_{eff}$  (or  $k_{ind}$ ) is consistent with the ability of the codes for flux and power distribution calculations. The 10 and 20 per cent criteria on the other quantities probably reflect what is thought to be possible with the present status of nuclear data and calculational methods rather than what is desirable. Improvements in the confidence level of these quantities might result in reduced safety margins. As to the prediction of isotopic composition of irradiated fuel, the precision of the calculation is very important for the determination of an economically optimal fuel management scheme; according to A. F. Henry<sup>5)</sup> millions of dollars could be saved for instance by changing the enrichment by 0.1 per cent at the right place if the calculations were sufficiently accurate to allow that place to be determined.

Reports on comparisons between the results obtained by "modern" calculations using the most recent fundamental nuclear data and the results of older codes with their respective cross sections most often show that the old programs agree best with experiments. This is quite natural, because over a long time the "not-fundamental" data accumulate experience in the solution of the specific problems they are intended for, and in many cases the data contain fittings which neutralize calculational errors in the reactor physics codes. Calculations based on fundamental nuclear data will, on the other hand, in many cases yield results for the integral reactor parameters outside the tolerated error limits mentioned above.

The fundamental nuclear data for reactor physics purposes are available as evaluated data libraries stored on magnetic tape in a form suitable for computer processing. When the data of these libraries fail to predict the reactor physics quantities with the accuracy wanted, the reason is that the

knowledge of some neutron cross sections, even in areas very important in reactor physics, is still too poor to allow the evaluators to select the correct data. In some areas measurements are impossible with the present status of technology, and in other cases two or more experimental methods which are judged to be equally good give discrepant results. A survey of the at present most troublesome discrepancies is given by J. J. Schmidt in ref. 6. For thermal reactor purposes the worst of the outstanding discrepancies is associated with the resonance capture integral of  $U^{238}$ ; the resonance integrals obtained from the best available sets of resonance parameters are about 10% higher than those found by the measurements of the average  $U^{238}$  capture cross sections. Some other discrepancies are serious in fast reactor calculations, but not very important for thermal systems, for instance those concerning the fission spectra for the main fissile nuclides and the energy dependence of  $\bar{\nu}$ . The  $\alpha$ -value for  $Pu^{239}$ , which is greatly energy-dependent, is also a source of trouble in fast reactor calculations.

An evaluated data set which is known to contain uncorrect data, partly caused by such well-known discrepancies, may be handled in different ways. One is to adjust the basic data by varying the cross sections in certain energy regions or by changing some of the resonance parameters until agreement is obtained with integral measurements. Another is to calculate integral parameters from the existing data and then introduce the corrections if necessary. The latter method is in use in France, West Germany, and the United Kingdom, whereas the former is used for instance in Sweden and the U. S. A.<sup>7)</sup> This fundamental disagreement makes the three main evaluated data libraries fall into two groups; in the evaluation of version III of the ENDF/B<sup>8)</sup> results from integral measurements are taken into consideration, whereas the evaluators of the KEDAK<sup>9)</sup> and the UKNDL<sup>1, 2)</sup> select the cross section values given by the best differential data.

The data generating code system described in this report is based on the following principles:

- (1) The basis is fundamental nuclear data; i. e. the evaluated data library UKNDL is used, supplemented with thermal scattering models and with resonance parameters for some important nuclides.
- (2) Updating should be possible as better knowledge of nuclear data is attained.
- (3) It is attempted as far as possible to create easy communication to the reactor physics codes which use the system as a data supply.

The fact that the UKNDL was chosen implies that fitting of the basic nuclear data was avoided. It seems to me, that the most commendable way of handling the unresolved data problems is to simply wait for their solution in a later version of the evaluated library, and in the meantime get through by means of experience concerning how far off and to which side the calculated results will lie. Only at one point is a correction introduced; the  $U^{238}$  resonance integral is reduced by the ad hoc formula described in section 3.2.

Some testing of the data-generating system has previously been performed in the calculations on the first core of the Dresden 1 boiling water reactor<sup>10)</sup>, in the benchmark calculations on homogeneous critical spheres performed by Neltrup<sup>11)</sup>, and in the lattice calculations presented at the Nordic Reactor Physics Meeting, November 1972 in Helsinki<sup>12)</sup>. At the moment a project with the purpose of testing the entire reactor physics code system at Risø is in progress; the calculation model is the Connecticut Yankee PWR, and the project tests the data system especially as regards its ability to predict the temperature coefficients<sup>13)</sup>. In this report test calculations involving a minimum of "foreign" codes will be presented; the purpose is to check the data system without the addition of uncertainties from the succeeding neutronics programs.

### 3. DATA SYSTEM DESCRIPTION

The task of the data system is to transform the various nuclear data into a form convenient for reactor physics calculations. This means that the data should be converted into effective group cross sections as the succeeding neutronics codes all involve multigroup flux solutions. The multigroup approach is used at all energies, as this method is more flexible than, for instance, one involving a pointwise representation of the thermalization region.

The sources of data fall into three main blocks, the MASTER TAPE, the resonance treatment, and the thermal scattering treatment. These three parts are combined by means of a program called CRS<sup>4)</sup>, which besides that sees to the cross section transfer to the user codes. The details of the cross section preparation will be described in the following sections of this chapter.

#### 3.1. The SIGMA MASTER TAPE

The SIGMA MASTER TAPE<sup>3)</sup> contains fine group cross sections for the materials available in the UKNDL, version 1968<sup>1, 2)</sup>, from which it was generated. The processing code used is SIGMA, for which only a preliminary report exists<sup>14)</sup>, but the program scope is very similar to that of GALAXY<sup>15)</sup>. The fine group structure is constructed on the theory that the groups should be fine enough for the cross sections to be applicable to all sorts of reactor calculations, but on the other hand the number of groups should not exceed what is practicable for a flux calculation. The MASTER TAPE will hence not need to be regenerated before an updating of the basic data is wanted.

From these criteria a 76-group structure was set up, the 76 groups spanning the energy range from  $10^{-10}$  to 15 MeV. Normally the 35 lowest-lying energy groups are regarded as thermal groups; the limit between fast and thermal is thereby fixed at 1.855 eV, as in the well-known cell program LASER<sup>16)</sup>. In fact, the 35 thermal groups are identical to those of LASER, with the gatherings of narrow groups around the thermal resonances of Pu<sup>239</sup> at 0.3 eV and of Pu<sup>240</sup> at 1 eV.

Scattering anisotropy is accounted for by the transport correction of Honeck<sup>17)</sup>, where the sum of the first-order Legendre coefficients for the scattering from a group is subtracted from the self-scattering term. This correction is used only for the elastic scattering cross section. The elastic and inelastic cross sections are combined into one scattering matrix, whereas the (n, 2n) and (n, 3n) processes are included in the fission cross section. Because of these processes the full fission matrix has been retained for the description of neutron production.

The group cross sections are stored in binary form on a magnetic tape. The production of the tape and the formats are described in ref. 3.

#### 3.2. Resonance Treatment

The data system is provided with resonance data from the RESAB Program System<sup>18, 19)</sup>. RESAB File 1 produces effective resonance cross sections either by semi-analytical methods from resonance parameters or by condensation of the detailed resonance cross sections with a flux spectrum obtained by a collision probability theory solution of the slowing-down equation in a very fine energy mesh. The cross section tables for the latter method can be calculated from resonance parameters in the multi-level routine DORES<sup>20)</sup>, which is part of the RESAB File 2 program. Alternatively the tabulations of the UKNDL may be used.



For normal calculations the resonance treatment includes the nuclides  $U^{235}$ ,  $U^{238}$ , and  $Pu^{239}$ . In the standard mode of producing the resonance cross sections, resonance parameters are used with DORES for the s-wave part of the  $U^{238}$  cross section in the energy region where resonances are resolved. For  $U^{235}$  and  $Pu^{239}$  the UKNDL data are used, as the resonance parameters of these nuclides are available only in a very limited low-energy interval. All UKNDL data are given at room temperature, but the contribution to the Doppler effect from fissile nuclides is not very important in thermal reactors. The detailed slowing-down calculation is then performed for the resolved region, and effective group cross sections are produced. In the unresolved region an analytical calculation based on statistical parameters is applied for  $U^{238}$ , and this is also the case for the p-wave contribution to the  $U^{238}$  cross section in the resolved region. The resulting effective resonance group cross sections are transferred via punched cards to the CRS code.

For the supply of one such set of group cross sections two RESAB-runs are necessary. First a cross section tape is produced in a RESAB File 2 run, and then the effective cross sections are prepared by RESAB File 1. To facilitate the resonance treatment the routine RESOREX<sup>21</sup>, developed by Neltrup, was incorporated in the CRS program.

In RESOREX interpolation is performed in tables of group resonance integrals calculated by RESAB as a function of two parameters, the temperature and the effective NR scattering cross section. The latter parameter is calculated from the unit cell specification by means of an equivalence principle, reducing the cell to an equivalent homogeneous mixture. The library for RESOREX contains group resonance integrals for  $U^{238}$  capture and for both capture and fission in  $U^{235}$  and  $Pu^{239}$ . Its generation by RESAB calculations is described in ref. 21. In the present version of the library the resonance integrals are tabulated at nine values of the NR scattering cross section, but at two temperatures only, 861 and 1200 K. It has been shown, however, that extrapolation in the square root of temperature even to room temperature gives accurate results. As demonstrated in ref. 21 the routine generally yields cross sections in good agreement with those calculated by RESAB.

The RESOREX treatment is limited to fuel rod cells, and the materials allowed are in the fuel  $U^{235}$ ,  $U^{238}$ , and  $Pu^{239}$ , for which effective resonance cross sections are produced, and O. RESOREX has an option for metal fuel, but the present library is valid only for oxide. The clad materials are Al, Zr, Fe, Ni, and Cr, and the moderator may contain H, D, C, and O.

If other materials are included in the cell description for CRS, they will simply be ignored by RESOREX.

Besides the group resonance cross sections, RESOREX calculates and prints the Dancoff correction factor for a uniform lattice. Two Dancoff factors are calculated; for one of them the cladding is considered as a NR scatterer, and for the other a WR scattering correction factor is applied (for details see ref. 21). Options are included in RESOREX for square and hexagonal cell Dancoff correction, but in CRS only the cylinder cell approximation can be activated. Finally RESOREX calculates some constants which are to be used in determining correction factors to the removal cross sections for the source depletion during slowing down through the resonance groups, as proposed by ASKEW<sup>22</sup>.

As deduced in ref. 22 a correction to the resonance group removal cross section for the fact that the flux decreases on the way down through a resonance group may be expressed as

$$f(p) = \frac{(1-p-\chi)\ln p}{(1-p)\chi\left(1 + \frac{\xi \ln p}{\tau}\right)}$$

Here

p is the escape probability of the group,

$\tau$  is the group lethargy width,

$\xi$  is the cell average mean logarithmic decrement, and

$\chi$  is the number of neutrons entering the group divided by the total number of neutrons slowed down past the upper energy limit. If the scattering nuclides are too heavy to make the neutrons skip the group completely,  $\chi = 1$ . Otherwise, if the group is narrow or the scattering material contains light nuclides, the value of  $\chi$  will be

$$\chi = 1 - \frac{\frac{E_u}{E_l} - \alpha + \alpha \ln \frac{\alpha E_u}{E_l}}{1 - \alpha + \alpha \ln \alpha}$$

where  $E_u$  and  $E_l$  are upper and lower energy boundary of the group, and  $\alpha$  is determined by

$$\alpha = \left(\frac{A-1}{A+1}\right)^2$$

A is the atomic weight of the scatterer. In the case of hydrogen  $\chi$  is expressed simply as

$$\chi = \frac{E_u - E_l}{E_u} .$$

This removal correction is in CRS calculated in all groups included in the RESOREX resonance treatment for the nuclides H and D only, although the correction is more significant for the heavier nuclides. The reason for this choice is that the hydrogen and deuterium isotopes are considered far the most important for the slowing down in water reactors. All of the out-scattering cross sections from a group are multiplied by the correction factor belonging to the group. This change is compensated for in the self-scattering term, the total cross section being left unaltered.

In the case of hydrogen the effect of the correction is a slight lowering of the removal cross section, causing a reduction of the calculated multiplication factor for usual rod lattices. For the Yankee reactor investigated in chapter 5 of this report the effect is approximately a 0.5% reduction in  $k_{eff}$ . The build-up of Pu isotopes is only slightly affected.

Burn-up calculations show that the resonance integral of  $U^{238}$  as calculated by RESAB from the present resonance parameter library is too high by about 10%, in accordance with the well-established discrepancy between differential and integral measurements of the  $U^{238}$  capture mentioned in chapter 2. This caused the only departure in the CRS cross section system from the principle of using only unfitted fundamental data. The resonance integrals of  $U^{238}$  in the groups where resolved resonances were used are simply reduced by the amounts calculated from the formula applied in WIMS<sup>23)</sup>:

$$\frac{A_1}{\tau} = 0.2 \left( 1 - \frac{3I}{2\sigma_p \tau} \right) \text{ barns.}$$

In this formula  $\tau$  is again the group lethargy width,  $\sigma_p$  is the effective NR scattering cross section of the RESOREX equivalence principle, and  $I$  is the corresponding group resonance integral.

This correction of course has the effect of making the multiplication factor higher and the production of  $Pu^{239}$  lower. In chapter 5 of this report it is demonstrated that the calculation results for the Yankee reactor are quite satisfactory with the correction applied. Burn-up calculations for the

Dresden<sup>10)</sup> also predicted the Pu build-up to a good accuracy. But no discussion of whether the 0.2 barn factor of the formula should perhaps be slightly higher or lower will be presented here, because the mere introduction of a such correction is in serious contravention of the basic principles of the data system. It is to be hoped that better knowledge of the data will soon make it unnecessary.

The resonance treatment so far is limited to the three nuclides  $U^{235}$ ,  $U^{238}$ , and  $Pu^{239}$ . For the calculations at high burn-up values or for calculations involving recycled fuel the higher Pu-isotopes ought to be included, at least the possibility of calculating the Doppler broadening of the  $Pu^{240}$  1 eV - resonance would be desirable. Furthermore, if for instance Th- $U^{233}$  systems should be treated, the resonance treatment would naturally have to be extended to include these isotopes as well.

### 3.3. Thermal Scattering

For the treatment of thermal scattering the routine NELKINSCM<sup>24)</sup> was first built into the CRS program. NELKINSCM is based on the Nelkin model for H in  $H_2O$  and a modified Nelkin model for D in  $D_2O$ . For other nuclides the free gas model is applied. The transfer probabilities are calculated from energy mid-point to energy mid-point of the thermal part of the fine group structure, and the transformation into group transfer cross sections is simply done by multiplying the transfer probability by the lethargy width of the receiving group. It appeared, however, that the upper part of the calculated thermal flux spectrum showed some strange oscillations where it was expected to fall off smoothly towards the epithermal level. An example of this abnormal picture is shown in fig. 4.4. a in section 4.4 of this report (dashed curve).

It was found that the effect was caused by the, in this respect, too broad groups of the MASTER TAPE group structure. Therefore it was decided to make another thermal scattering routine, NELLY<sup>25)</sup>, which was to use a library generated by NELKINSCM in a greater number of groups.

The NELLY library was made in the following way:

First scattering matrices were produced in a 205-group thermal structure at a number of temperatures for the materials H, D, and a number of selected values of atomic weight. This calculation was a rather time-consuming computer task. The 205-group data were condensed to the 35 thermal MASTER TAPE groups by assuming a Maxwell thermal flux, and the 35-group data were fitted by polynomial expressions with the parameters atomic mass and temperature. The coefficients of these polynomials were

stored in the NELLY library.

The thermal spectrum obtained by using the NELLY cross sections looks more reasonable (fig. 4.4.a). Besides the NELLY routine only performs a simple interpolation, and it is therefore much faster than NELKINSCM. However, as is also demonstrated in chapter 4, the calculated  $k_{\text{eff}}$  is very insensitive to the thermal scattering data, so the previously reported results, for instance of the Dresden calculations<sup>10)</sup>, where NELKINSCM was used are still valid.

The NELKINSCM and NELLY routines may be used for H<sub>2</sub>O and D<sub>2</sub>O moderators and for all materials for which the free atom model is a good approximation. But for a graphite moderator, for instance, they are inadequate. Therefore the thermal scattering code FLANGE II<sup>26)</sup>, which processes the thermal data from the ENDF/B<sup>8)</sup> library, was imported. Unfortunately the scattering law data files of the ENDF/B have not yet been released<sup>27)</sup>; only the materials Be and BeO are available, and therefore the work with FLANGE II has been suspended for the time being.

### 3.4. The CRS Program

The combination of the MASTER TAPE data, the thermal scattering data, and the resonance data is done by the CRS program<sup>4)</sup>. This program also contains flux solution routines which perform the flux spectrum calculation in the fine-group structure (76 groups) and condensation routines which produce few-group cross sections by condensation with the calculated spectrum. Output options corresponding to the programs most commonly used are available.

Two flux solution routines are found in the present version of the program. One of them is a zero-dimensional routine, which is able to search for criticality by varying one of the three parameters  $k_{\text{eff}}$ , the buckling, or a poison specified by its absorption cross section. A group-dependent buckling may be used. Naturally this routine is used for homogeneous problems, but it may be useful in some heterogeneous cases too, where the spatial spectrum variation is not too important, for instance if condensation is performed only into 10 or more groups, the necessary number of condensed groups being, of course, dependent upon the nature of the problem.

The other flux routine is one-dimensional and uses collision probability theory for determining the flux and the  $k_{\text{inf}}$  and  $k_{\text{eff}}$ . A group-dependent buckling may be applied; it is only used for determining the  $k_{\text{eff}}$  and will

not affect the calculated flux. The boundary conditions are specified as greyness, which may also be group-dependent.

The one-dimensional routine is used when cross sections for unit cells are to be produced, and it is very suitable for cells which may be regarded as asymptotic, for instance usual PWR cells. It is also used when few-group data for water gaps and structural materials are wanted; in such cases a fuel zone is made by cell homogenization, and for instance a slab geometry spectrum is calculated (in the case of a water gap surrounding a BWR box).

For BWR spectrum calculations it is impossible to define an asymptotic unit cell because of the great influence on the spectrum from the water between the boxes. It has appeared, however, that reasonably good results are obtained by using the homogeneous spectrum for the condensation to 10 groups<sup>10)</sup>, in other words the 10-group system is a sufficiently fine energy division to make the condensed cross sections rather insensitive to the spatial variation of flux within the cell. A better approximation in the BWR case would probably be to apply the cluster geometry routine MAMIC<sup>28)</sup> to the flux solution; by transformation of the BWR box into an annular cluster surrounded by a water zone, the spectrum influence from the water gap could be accounted for. So a natural further development of the CRS program would be to build into it the MAMIC routine, and if the problems are limited to four material regions, the flux solution will presumably be possible even in the 76-group structure.

### 3.5. Communication to the Reactor Physics Programs Using the Cross Section Data

The condensed cross sections from CRS proceed to other codes where as a principal rule a better spatial description replaces the fine energy solution. In a typical calculation the next stage code will be the box burn-up program CDB<sup>29,30)</sup>. The unit cell burn-up part of CDB, called CEB, is available as a separate code which is used for the Yankee reactor calculations described in chapter 5 of this report. From CDB the data, now in the form of homogenized box average cross sections, are transferred to the overall calculation programs, the two-dimensional TWODIM<sup>29)</sup>, or the three-dimensional SYNTRON<sup>32)</sup>. This is the usual way through the program complex; besides the CRS program contains options for producing cross sections for the one-dimensional S<sub>n</sub>-code DTF IV<sup>33)</sup> (used for the calculations of chapter 4), the two-dimensional S<sub>n</sub>-code TWOTRAN<sup>34)</sup>, and the collision probability theory code CELL<sup>29)</sup>.

The most commonly used group structures are shown in table 3.5.a as subsystems of the 76 fine-group structure. The fine-group structure is described in detail in ref. 3. Cell burn-up calculations are normally performed in the 10-group structure; the 5- and 2-group systems are used for the box and overall flux solutions. The 10 burn-up groups have previously been demonstrated to be adequate for reactor calculations (see refs. 10 and 29), and besides it is not easy to switch over to another system because the fission product data of the burn-up codes are developed for these 10 groups (CEB-FIPO, ref. 31). The energy group description in the overall calculations is more flexible; the number of groups applied here depends upon how many spatial meshes are wanted, i. e. how many flux points in total the computer is able to handle.

Table 3.5.a.

Group structures expressed in fine-group numbers

76-group structure	10-group structure	5-group structure	2-group structure
41 fast groups	4 fast groups containing the fine groups 1 - 13	3 fast groups containing the fine groups 1 - 13	1 fast group containing the fine groups 1 - 41
	14 - 26	14 - 26	
	27 - 30	27 - 41	
	31 - 41		
Limit between fast and thermal: 1.855 eV			
35 thermal groups	6 thermal groups containing the fine groups 42 - 47	2 thermal groups containing the fine groups 42 - 55	1 thermal group containing the fine groups 42 - 76
	48 - 52	56 - 76	
	53 - 55		
	56 - 63		
	64 - 70		
	71 - 76		

#### 4. CALCULATIONS ON HOMOGENEOUS CRITICAL SPHERES

In most of the calculations which may be undertaken to test the reliability of a data system neutronics codes with all their uncertainties and approximations are involved. This of course makes it difficult to tell if an eventual error is due to inaccurate cross sections. For that reason measurements on simple geometry assemblies are desirable, for instance homogeneous spherical systems, for which an accurate one-dimensional transport calculation should determine the flux and reactivity as well as allowed by the applied cross sections.

For the testing of the data system two sets of such critical experiments were selected, both of them "clean", i. e. well documented with all information needed for the calculations. Both sets concern spherical reactors for which diameters, material contents, and measured  $k_{eff}$  (about 1) are given. For each of the spheres  $k_{eff}$  was calculated by the most accurate methods possible and compared with the experimental value. The two series of experiments are the critical uranium-fuelled spheres of Gwin and Magnuson<sup>35,36</sup> at ORNL and the bare spherical systems from the Pu experiments performed at Hanford by Kruesi et al.<sup>37</sup>. Three of the spheres from each of these series have been used by Slaggie<sup>38</sup> for checking the data of the ENDF/B<sup>8</sup> versions 1 and 2, and the same six spheres were proposed by Neltrup as a benchmark calculation at the Nordic Reactor Physics Meeting at Risø, November 1971. The Neltrup's calculations are reported in ref. 11.

About the value of benchmark calculations on such geometrically simple assemblies it might be said that good agreement between theory and experiment in these cases by no means guarantees that the data system is applicable to for instance light-water reactor calculations. But combined with test calculations for relevant light-water lattices they may give an indication of whether or not eventual good agreement is due to cancelling out of errors, and this again is important for the reliability of the system in changing to a different reactor type. Unfortunately only very limited parts of the data system are checked; in this case where dilute aqueous solutions of high-enrichment fuel are used, especially the water scattering kernel and the thermal cross sections of U<sup>235</sup> and Pu<sup>239</sup> are important, whereas the epithermal data only slightly affect the reactivity because of the very effective moderation.

4.1. U<sup>235</sup> Spheres

The critical experiments of Gwin and Magnuson<sup>35,36)</sup> include eleven U<sup>235</sup> and U<sup>233</sup> fuelled reactors consisting of a spherical aluminium shell filled with a light-water solution of uranyl nitrate and different concentrations of boric acid. These experiments have been carefully analysed by Staub et al. in ref. 39 where corrections to the measured eigenvalues are found for effects such as the reactivity value of the shell and the neutron reflection of the room. The influence on the eigenvalue of the distortion from spherical shape of the containers is shown to be negligible. Furthermore the reported eigenvalues, obtained by period measurements, are corrected for the applied value of the delayed neutron fraction which was slightly lower than the more recent values. The experimental uncertainty in isotopic composition is estimated as corresponding to  $\pm 1\%$  on  $k_{eff}$ .

Of the eleven critical experiments, six were fuelled with U<sup>233</sup>. These experiments were excluded from the present calculations, because the purpose of this work is primarily to check the data with reference to U<sup>235</sup> light-water systems, and no resonance treatment for U<sup>233</sup>-Th fuel has been built into the CRS program. The remaining spheres were experiments Nos. 1, 2, 3, and 4 with a radius of 34.595 cm, and experiment No. 10 with radius 61.011 cm. Experiments Nos. 1 and 10 had no admixture of boron; in the rest of the smaller spheres the boron content and consequently the fuel concentration was gradually increased, which permits an eventual systematic error due to the boron absorption cross section to be investigated.

In table 4.1. a the data needed for the  $k_{eff}$  calculation are listed. The number densities for the five compositions are taken from ref. 36, except for the oxygen number density, which is calculated in ref. 39 from the chemical compounds in the solutions. Table 4.1. b gives the measured eigenvalue reported in refs. 35 and 36 together with the eigenvalue obtained after the corrections of ref. 39 have been used. The corrected measured eigenvalue is to be compared with the calculated one. All experiments were performed at a temperature of 293 K.

Table 4.1. a

Number densities and radii of ORNL spheres

Experiment No.		1	2	3	4	10
radius (cm)		34.595	34.595	34.595	34.595	61.011
Number densities (10 <sup>24</sup> cm <sup>-3</sup> )	B	0	5.2 <sub>10</sub> <sup>-6</sup>	1.04 <sub>10</sub> <sup>-5</sup>	1.28 <sub>10</sub> <sup>-5</sup>	0
	H	0.066228	0.066148	0.066070	0.066028	0.066394
	O	0.033736	0.033800	0.033865	0.033902	0.033592
	N	1.869 <sub>10</sub> <sup>-4</sup>	2.129 <sub>10</sub> <sup>-4</sup>	2.392 <sub>10</sub> <sup>-4</sup>	2.548 <sub>10</sub> <sup>-4</sup>	1.116 <sub>10</sub> <sup>-4</sup>
	U <sup>234</sup>	5.38 <sub>10</sub> <sup>-7</sup>	6.31 <sub>10</sub> <sup>-7</sup>	7.16 <sub>10</sub> <sup>-7</sup>	7.62 <sub>10</sub> <sup>-7</sup>	4.09 <sub>10</sub> <sup>-7</sup>
	U <sup>235</sup>	4.8066 <sub>10</sub> <sup>-5</sup>	5.6206 <sub>10</sub> <sup>-5</sup>	6.3944 <sub>10</sub> <sup>-5</sup>	6.7959 <sub>10</sub> <sup>-5</sup>	3.6185 <sub>10</sub> <sup>-5</sup>
	U <sup>236</sup>	1.38 <sub>10</sub> <sup>-7</sup>	1.63 <sub>10</sub> <sup>-7</sup>	1.84 <sub>10</sub> <sup>-7</sup>	1.97 <sub>10</sub> <sup>-7</sup>	2.20 <sub>10</sub> <sup>-7</sup>
U <sup>238</sup>	2.807 <sub>10</sub> <sup>-6</sup>	3.281 <sub>10</sub> <sup>-6</sup>	3.734 <sub>10</sub> <sup>-6</sup>	3.967 <sub>10</sub> <sup>-6</sup>	1.985 <sub>10</sub> <sup>-6</sup>	

Table 4.1. b

Experimental eigenvalues of ORNL spheres

Experiment No.	1	2	3	4	10
Measured $k_{eff}$	1.0018	1.0073	1.0090	1.0028	1.00129
Corrected $k_{eff}$	1.00026	0.99975	0.99994	0.99924	1.00031

4.2. Pu Spheres

A large number of critical experiments with aqueous Pu solutions performed at Hanford are reported by Kruesi et al.<sup>37)</sup> One of the experimental series, the nitrate experiments, was chosen for the calculations. In these series the reactors were unreflected stainless-steel spheres of two sizes where a solution of nitric acid was brought to criticality by gradual adding of plutonium nitrate in small amounts. The critical concentration of plutonium is varied by different concentrations of nitrate and a small addition of iron. For each of the experiments the concentrations were determined for a composition just above and one just below criticality so that the reported concentrations, obtained by interpolation between the two states, should be those of the exactly critical conditions.

The reactors had nominal diameters of 16 and 18 inches respectively, and the walls of the spheres were 0.050 inches SS 347. The 18-inch reactor was covered by a 0.020-inch layer of cadmium. The effective radii of the reactors to be used for the calculations were obtained by measuring the reactor volumes.

In table 4.2. a the number densities and temperatures for the 18-inch spheres are given, and in table 4.2. b the corresponding data for the 16-inch experiments.

Table 4.2. a  
Data for Hanford 18-inch spheres

Experiment No.	1	2	3	4	5	6
H	0.064954	0.064535	0.064296	0.063400	0.062504	0.060412
N	$7.3941 \cdot 10^{-4}$	$9.4971 \cdot 10^{-4}$	$10.4695 \cdot 10^{-4}$	$14.4162 \cdot 10^{-4}$	$19.3459 \cdot 10^{-4}$	$27.7570 \cdot 10^{-4}$
O	0.034440	0.034762	0.034884	0.035426	0.036218	0.037286
Fe	$1.2942 \cdot 10^{-6}$	$1.3589 \cdot 10^{-6}$	$1.4559 \cdot 10^{-6}$	$1.3265 \cdot 10^{-6}$	$1.4775 \cdot 10^{-6}$	$1.5207 \cdot 10^{-6}$
Pu <sup>239</sup>	$5.3932 \cdot 10^{-5}$	$5.6466 \cdot 10^{-5}$	$5.5839 \cdot 10^{-5}$	$5.7552 \cdot 10^{-5}$	$6.0761 \cdot 10^{-5}$	$6.6311 \cdot 10^{-5}$
Pu <sup>240</sup>	$2.3546 \cdot 10^{-6}$	$2.4652 \cdot 10^{-6}$	$2.4378 \cdot 10^{-6}$	$2.5126 \cdot 10^{-6}$	$2.6527 \cdot 10^{-6}$	$2.8950 \cdot 10^{-6}$
Temperature (K)	295	295	293	294	296	294
Measured volume 49.0 litres corresponding to an effective radius of 22.70 cm. Reactor wall 0.127 cm SS 347 covered with 0.0508 cm cadmium.						

Table 4.2. b

Data for Hanford 16-inch spheres

Experiment No.		7	8	9	10	11
Number densities (10 <sup>24</sup> cm <sup>-3</sup> )	H	0.064117	0.064057	0.063878	0.062563	0.060293
	N	10.1412 <sub>10</sub> <sup>-4</sup>	10.6268 <sub>10</sub> <sup>-4</sup>	15.8334 <sub>10</sub> <sup>-4</sup>	17.4847 <sub>10</sub> <sup>-4</sup>	27.3733 <sub>10</sub> <sup>-4</sup>
	O	0.034771	0.034870	0.036092	0.035848	0.037210
	Fe	1.1216 <sub>10</sub> <sup>-6</sup>	1.2942 <sub>10</sub> <sup>-6</sup>	1.3373 <sub>10</sub> <sup>-6</sup>	1.9197 <sub>10</sub> <sup>-6</sup>	1.9305 <sub>10</sub> <sup>-6</sup>
	Pu <sup>239</sup>	8.4001 <sub>10</sub> <sup>-5</sup>	8.7429 <sub>10</sub> <sup>-5</sup>	9.2474 <sub>10</sub> <sup>-5</sup>	9.2088 <sub>10</sub> <sup>-5</sup>	10.4278 <sub>10</sub> <sup>-5</sup>
	Pu <sup>240</sup>	3.6400 <sub>10</sub> <sup>-6</sup>	3.7886 <sub>10</sub> <sup>-6</sup>	4.0072 <sub>10</sub> <sup>-6</sup>	3.9904 <sub>10</sub> <sup>-6</sup>	4.5187 <sub>10</sub> <sup>-6</sup>
Temperature (K)		296	297	297	296	295
Measured volume 34.15 litres corresponding to an effective radius of 20.1265 cm.						
Reactor wall 0.127 cm SS 347						

### 4.3. Methods of Calculation

In order to do the flux and  $k_{\text{eff}}$  calculations as accurately as possible and because of the very limited size of the assemblies the one-dimensional  $S_n$  program DTF IV<sup>33)</sup> was used. The order of the  $S_n$  calculation was taken to be  $S_8$ , and a flux calculation mesh of 25 space points was applied in the fuel mixture, distributed in the same way as reported by Neltrup<sup>11)</sup>. Two meshes were added in the stainless-steel wall for the Pu spheres and one for cadmium in the cases where the cadmium cover was present. The eigenvalues of the U spheres have been corrected for the wall effect and therefore their shells were neglected. As shown by Neltrup<sup>11)</sup> by variation of the number of meshes and the  $S_n$  order, the 25 space points and the  $S_8$  approximation are sufficient for these calculations. As the DTF IV program is very slowly converging for this type of problems, the very strict convergence criterion of  $10^{-6}$  on the eigenvalue was used in order to guarantee properly converged results.

The cross sections for the transport calculations were produced in the DTF IV format by CRS. The standard 10-group structure was used (see

section 3.5). For the condensation to 10 groups a homogeneous 76-group spectrum for the fuel mixture was calculated, assuming a group-dependent buckling given by

$$B_g^2 = \frac{\kappa^2}{(R + 0.71/\Sigma_{\text{tr},g})^2},$$

where  $B_g^2$  is the buckling term in group  $g$ ,  $R$  the sphere radius, and  $\Sigma_{\text{tr},g}$  the macroscopic transport cross section of the group. By this procedure a first guess of the eigenvalue is at the same time obtained from the CRS program.

Resonance cross sections for  $U^{235}$ ,  $U^{238}$ , and  $Pu^{239}$  were supplied from the RESAB program<sup>19)</sup>. Because of the very small concentrations the infinitely dilute group cross sections of the MASTER TAPE might have been used, but as these data will never be used in a "realistic" reactor calculation, testing of them would hardly be worth-while. The examination of the RESAB cross sections is more interesting, even in the limit of infinite dilution.

For the stainless-steel wall and the cadmium cover cross sections were condensed with the spectrum calculated for one of the fuel mixtures. Although this spectrum corresponds better to the centre of the sphere than to the shell, these cross sections are thought to be sufficiently accurate, as the reflection effect of the wall implies only a small correction of the eigenvalue.

The main difference in calculational method between the present calculations and those of Neltrup for six of the cases<sup>11)</sup> is that the NELLY procedure has now become operational and has been used for the thermal scattering data instead of the old version of NELKINSCM used by Neltrup. With its library on the basis of 205 thermal groups the NELLY routine should give a more accurate treatment of the thermalization. In addition the convergence criterion was made a factor of ten stricter - giving an eigenvalue only about 0.05 per cent higher. The cadmium cover accounted for here was omitted in Neltrup's calculations; its reflection raises  $k_{\text{eff}}$  by a small amount for the 18-inch diameter Pu spheres.

For the ENDF/B test calculations of Slaggie<sup>38)</sup> a transport code very similar to DTF IV was used. The ENDF/B and the Risø results should therefore be directly comparable.

#### 4.4. Results of Sphere Calculations

Calculations for some of the spheres with an earlier version of the CRS program are reported by Neltrup<sup>11)</sup>. The most important difference from the present calculations is the thermal scattering treatment which in the calculations of Neltrup was performed by an old and inaccurate version of the procedure NELKINSCM. This procedure has now been replaced by the interpolation routine NELLY (see section 3.3), and as the homogeneous spheres are very well-moderated assemblies, they were expected to be sensitive to the thermal scattering cross sections. In fact, the work of Slaggie<sup>38)</sup> was undertaken particularly to test the light-water thermal scattering data of the ENDF/B.

In fig. 4.4.a the thermal spectrum as calculated in the CRS code for ORNL sphere No. 1 is shown together with the spectrum obtained by using the old NELKINSCM version. The spectra are somewhat arbitrarily normalized to the same value in group No. 69. It is seen that the spectrum of the new calculations is slightly harder and that the small oscillations in the epithermal part due to a random nature of the transfer cross sections have vanished. (The dip at 1.14 eV is caused by a resonance in U<sup>235</sup>). But although very great differences exist between the two sets of thermal transfer cross sections, the spectrum seems to be relatively unaffected, indicating that the system is rather insensitive to the thermal scattering kernel. The CRS calculated  $k_{\text{eff}}$  for the sphere was lowered by only 2 per mille because of the spectrum hardening.

The results for the U<sup>235</sup>-fuelled ORNL spheres are listed in table 4.4.a. Together with the calculated  $k_{\text{eff}}$ 's the deviation from the corrected measured ones are given and for comparison the results of Neltrup<sup>11)</sup> and the ENDF/B version I and II results of Slaggie<sup>38)</sup>. The calculated values are a bit low compared with the experiments, and the agreement is slightly worse than in the calculations of Neltrup. As seen from fig. 4.4.a the main part of the thermal flux falls within the two lowest energy groups of the 10-group structure, and in order to examine the influence of this possibly unfavourable distribution of groups a 14-group calculation for sphere No. 1 was set up where each of the two groups were split into three. By this the  $k_{\text{eff}}$  was raised by about 0.002, leaving an error just below the magic limit of 1%.

Table 4.4.a

Eigenvalues for ORNL spheres

Experiment No.	1	2	3	4	10
Corrected measured	1.00026	0.99975	0.99994	0.99924	1.00031
CRS	0.9786	0.9782	0.9752	0.9766	0.9878
DTF IV	0.9894	0.9895	0.9867	0.9883	0.9903
Deviation from measurement	-0.01086	-0.01025	-0.01324	-0.01094	-0.01001
DTF IV, 14 groups	0.9915				
Neltrup, ref. 11	0.9927			0.9907	0.9940
ENDF/B I } ref. 38	0.9928			0.9928	0.9930
ENDF/B II }	0.9881			0.9881	0.9877

In fig. 4.4.b the deviation between the corrected measured and the calculated eigenvalue,  $\Delta k$ , is shown for the five cases, plotted as a function of the U<sup>235</sup> concentration. The ENDF/B calculations for three of the spheres are also shown. Care should be taken in the comparison with the ENDF/B as another data handling method was used in these calculations, and it is shown that the results are sensitive at least to the group structure, but a first impression is that the two data systems give results which are very much alike. The calculation with the CRS cross sections falls between the two ENDF/B calculations in the three cases.

The five points calculated are distributed around a mean value of  $\Delta k = -0.0111$  with deviations corresponding to the experimental uncertainty of  $\pm 1/4\%$ . It seems difficult to deduce anything concerning data inconsistencies from these points as no certain dependence on the boron content or the sphere size is shown. Perhaps a slight tendency of  $k_{\text{eff}}$  to decrease with increasing U<sup>235</sup> concentration is indicated, an impression which is emphasized by the opposite trend of the ENDF/B results.

The calculated eigenvalues of the Hanford Pu spheres are given in tables 4.4.b and 4.4.c for the 18- and 16-inch spheres respectively. The two sets of ENDF/B results and the results of Neltrup are shown as well. Again the improved treatment of the thermalization caused a slight worsening of the agreement with experiment, but here the calculated values are too



high. The ENDF/B gives even higher results with very little difference between the two versions.

Table 4.4.b

Calculated eigenvalues for Hanford 18-inch spheres

Experiment No.	1	2	3	4	5	6
CRS	0.9745	0.9822	0.9772	0.9765	0.9808	0.9831
DTF IV	1.0027	1.0108	1.0057	1.0051	1.0098	1.0128
Neltrup, ref. 11	1.0005					1.0101
ENDF/B I } ref. 38	1.0076					1.0167
ENDF/B II }	1.0082					1.0171

Table 4.4.c

Calculated eigenvalues for Hanford 16-inch spheres

Experiment No.	7	8	9	10	11
CRS	0.9848	0.9912	0.9988	0.9867	0.9861
DTF IV	1.0194	1.0261	1.0336	1.0219	1.0222
DTF IV, harder fission spectrum					1.0055
Neltrup, ref. 11					1.0201
ENDF/B I } ref. 38					1.0266
ENDF/B II }					1.0266

In fig. 4.4.c the difference between calculated and measured eigenvalues for the Hanford spheres is plotted as a function of the concentration of Pu<sup>239</sup> (the measured values are 1 in all cases). The points are more dispersed than for the ORNL spheres. That part of this effect is due to experimental uncertainty is seen by comparison of the number densities of for instance spheres 9 and 10 with calculated eigenvalues of 1.0336 and 1.0219 respectively (tables 4.2.b and 4.4.c). In going from experiment No. 9 to experiment No. 10 the concentration of both iron and nitrate is raised by small amounts, but the measured Pu concentration is decreased to give the difference in calculated values of  $k_{eff}$  for the two spheres of about 1 per cent. Apart from this scattering the results fall into two groups corresponding to the two reactor sizes. The mean value of the calculated eigenvalues for the larger spheres is 1.0078 which is rather good, whereas for the small ones it is 1.0246 which is unacceptable.

The excessive calculated reactivity might be explained by absorbing impurities in the fuel mixture. Some of the experiments of ref. 37 were analysed for impurities, but these were not. However, it seems unlikely that the influence of impurities should be so dependent upon reactor dimensions. Distortion of the shells from spherical shape might lower the measured reactivity in relation to what is calculated on the assumption of an ideal sphere. In the case of the ORNL spheres it has been shown<sup>39)</sup> that a departure from sphericity of just under 1 per cent in the diameter is quite unimportant. For the Hanford spheres the measured volumes are in good agreement with the nominal diameters so that no basis is found for the assumption that an important distortion should exist here.

Consequently the reason for the discrepancy must be sought in the calculations and most likely in the Pu data. The conclusion of Slaggie<sup>38)</sup> that in particular the thermal cross sections of the ENDF/B for Pu<sup>239</sup> should be suspected cannot explain the strong dependence on reactor dimensions. One thing which could give such a dependence is an error in the fission spectrum because of the very important leakage of the fast neutrons in the small systems. An examination of the fission spectra of U<sup>235</sup> and Pu<sup>239</sup> in the ten groups showed somewhat surprisingly that they are almost identical in the UKNDL data. Presumably the fission spectrum of Pu<sup>239</sup> should be harder.

To check if the calculated  $k_{eff}$  of the spheres is sensitive to the fission spectrum a test run with a different spectrum was made for one of the small spheres, No. 11. In the 10-group structure which was used for the calculations the fission spectrum falls in groups Nos. 1 and 2. The harder spectrum

was constructed simply by adding 0.05 to the spectrum value in the first group and subtracting the same amount in the second. The effect was a lowering of  $k_{eff}$  from 1.0222 to 1.0055, showing that the hardness of the fission spectrum has a great influence for these systems.

The eigenvalue calculations for the homogeneous spherical reactors were undertaken to test some essential parts of the data library, especially the thermal cross sections of  $U^{235}$  and  $Pu^{239}$  and the thermal scattering treatment for light water. The results for the uranium systems proved pretty satisfactory, considering the uncertainties in the calculation. The calculated eigenvalues were systematically slightly too low, but seemed to increase with a finer energy group division. In the judgement of the deviation it should also be borne in mind that it was not investigated whether the transport correction over- or underpredicts the scattering anisotropy of the systems.

As to the Pu spheres the agreement is generally worse. But it seems that the error might be due to the fission spectrum of  $Pu^{239}$ , and if this is the case, the situation is not too bad for normal uranium-fuelled light-water reactors where the leakage is less important, and in addition the concentration of  $Pu^{239}$  is small compared with that of  $U^{235}$  at moderate burn-up values.

Finally, with regard to the thermal scattering kernel, it may only be concluded that the calculated eigenvalues are very insensitive. The individual thermal group transfer cross sections are very different in the calculations of Neltrup<sup>11)</sup> and in the present ones, but nevertheless the eigenvalues only differ by a few per milles.

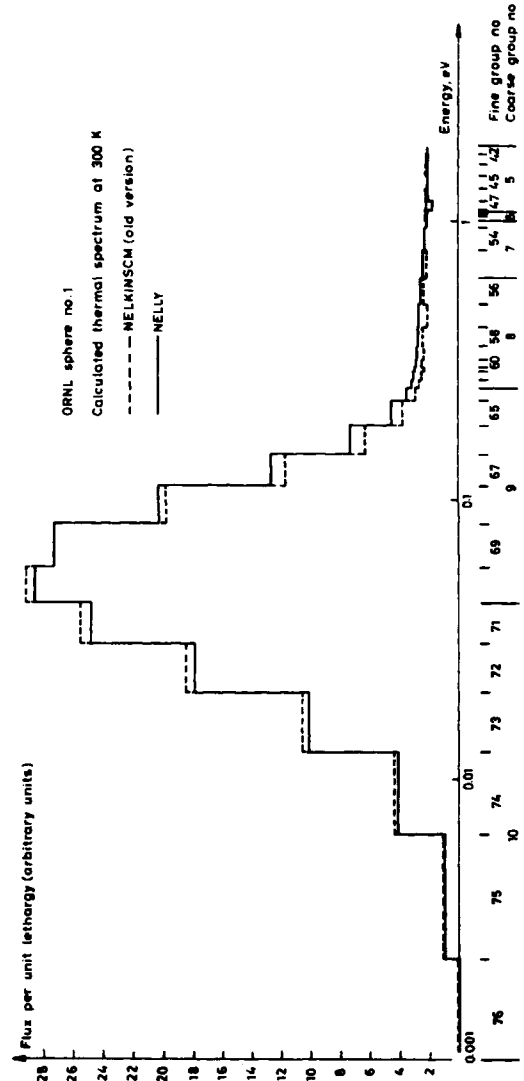


Fig. 4.4.a. CRS-calculated thermal flux for uranium-fuelled sphere

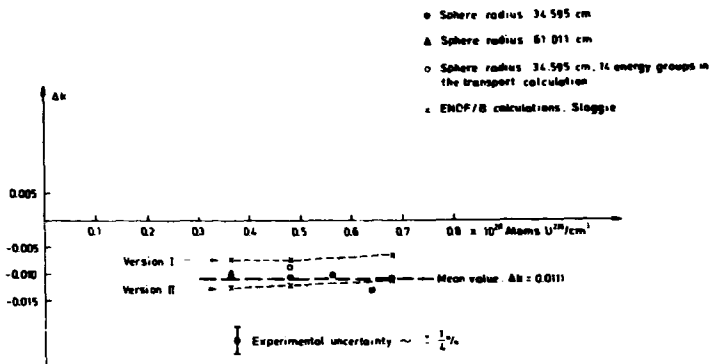


Fig. 4.4. b. Difference between calculated and corrected measured eigenvalues for ORNL spheres as a function of the  $U^{235}$  concentration

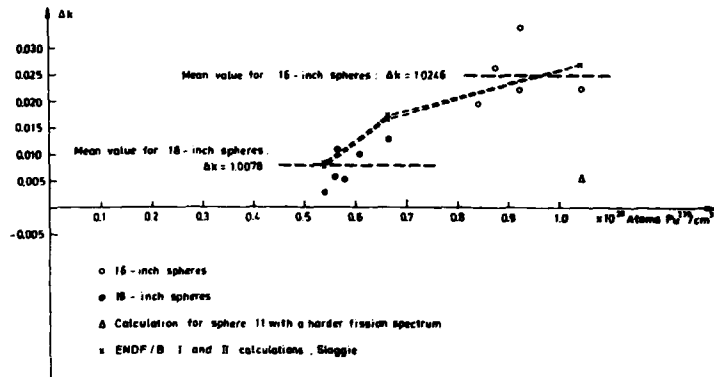


Fig. 4.4. c. Difference between calculated and measured eigenvalues for Hanford spheres as a function of the  $Pu^{239}$  concentration

## 5. UNIT CELL BURN-UP CALCULATIONS FOR THE YANKEE ROWE REACTOR

An accurate prediction of the production and destruction of heavy isotopes during burn-up is necessary for estimating the lifetime of a power reactor fuel loading and consequently for the predetermination of fuel costs. For the establishment of a fuel management strategy giving the optimal fuel performance it is also important to be able to calculate the isotopic composition of irradiated fuel. The accuracy of burn-up calculations is of course greatly dependent upon the quality of the data library used; especially the cross sections of the uranium and plutonium isotopes greatly influence the calculated isotope inventories of the spent fuel. To gain confidence in the data system with respect to the isotopic burn-up calculations one must check the data by comparison with mass-spectrometric analyses of the composition for fuel irradiated to high burn-up values.

The MASTER TAPE - CRS system has previously been used for burn-up calculations on the first core of the Dresden I reactor with fairly good results<sup>10)</sup>. For the Dresden I measurements of isotopic composition are available for exposures until about 20,000 MWD/TU; the bulk of the data, however, have burn-up values between 0 and 10,000 MWD/TU. As the Dresden reactor is a boiling water reactor no really asymptotic spectrum exists, and the burn-up calculations had to be performed at the box level with the consequence that the testing of the cross section data is veiled by the calculational inaccuracies of the box code. So the Dresden burn-up calculation is more of a check of the entire complex MASTER TAPE - CRS - CDB than simply of the data generating system.

For the Yankee reactor situated at Rowe, Massachusetts, measurements of isotopic compositions of spent fuel have been published for burn-up values until 46,000 MWD/TU. The Yankee reactor, being a PWR, has fuel boxes containing 304 or 305 fuel rods, and therefore the interior rods of the boxes are irradiated in a flux spectrum which to a good approximation is independent of the influence from water gaps and control rods. For the burn-up calculations on such interior rods a simple asymptotic pin cell code is sufficient. The Yankee measurements have been compared with *Risø* calculations before<sup>29)</sup>, but at that time the cross sections from the *LASER*<sup>16)</sup> library were used.

It may perhaps be true that the old-fashioned design of the Yankee core makes the reactor unfit for testing of a code system intended for use on modern power reactors. But for natural reasons measurements on modern

reactors at high burn-up values are not available, and furthermore the results of the experimental investigations of the Yankee core have been fully published thanks to a series of programs under contract between the Westinghouse Atomic Power Division and the U.S. Atomic Energy Commission. Most of the measurements for commercial reactors are classified, so, despite its drawbacks, the Yankee reactor still seems to be the best object for an evaluation of the reliability of a data system for burn-up purposes.

The present calculations check the cross section data of the heavy isotopes, in particular the ratios of cross sections for the different nuclides. But also the calculated spectrum influences the isotopic build-up, so the data for all the components of the fuel cell are important. It was the intention by means of these calculations to try to reach a conclusion concerning the optional resonance correction to the H removals and the ad hoc reduction of the  $U^{238}$  group resonance integrals described in section 3.2 of this report. The pin cell burn-up code CEB to be used for the calculations has been shown to work satisfactorily in the work of K. E. Lindstrøm Jensen<sup>29)</sup>.

### 5.1. The Yankee Core and the EYC Project

The Yankee nuclear power plant was started up in August 1960 and was operated at the nominal full power, 392 MWt, for the first time in January 1961. The reactor is a PWR of Westinghouse construction, and the core l description is found in ref. 40. Initial fuel composition was taken from ref. 41. Here only the data of importance to the present burn-up calculations will be given.

The Yankee initial core contains a total of 76 fuel elements with a fuel length of 233 cm. The entire core can be approximated by a cylinder with the diameter 191 cm. Each fuel element is composed of 9 subassemblies with 6 x 6 fuel rods giving a total of 18 x 18 rods in the element, but at the edges of the elements some fuel rods have been omitted to save space for the blades of the cruciform control rods or their zirconium followers, and at the centre one empty rod position forms an instrumentation channel. The number of rods for a fuel element is then 305 for the element type A and 304 for the element type B. The fuel element types A and B are shown in fig. 5.1. a. In table 5.1. a the core data needed for the unit cell calculations are listed.

Under the Yankee core evaluation program, the EYC project<sup>41, 42)</sup>, spent fuel from the Yankee core l was analysed for isotopic composition

Table 5.1. a

Yankee reactor core data (dimensions and densities refer to cold conditions)

Average core diameter (cm)	190.75
Active core height (cm)	233.40
Nominal system pressure (atm)	136
Nominal specific power (kW/kg U)	18.75
Fuel rod pitch (cm)	1.0719
Fuel rod outside diameter (cm)	0.8636
Cladding thickness (cm)	0.0533
Fuel pellet diameter (cm)	0.7468
Moderator temperature (°C)	268
Average clad temperature (°C)	280
Average fuel temperature (°C)	578
Fuel material	UO <sub>2</sub>
Fuel enrichment (w/o U <sup>235</sup> )	3.40
Average density of UO <sub>2</sub> (g/cm <sup>3</sup> )	10.18
Initial uranium fuel loading (kg)	20908
U <sup>234</sup> loading (kg)	4.1
U <sup>235</sup> loading (kg)	711
U <sup>236</sup> loading (kg)	4.1
U <sup>238</sup> loading (kg)	20188
Cladding material	Type 348 SS
Density of SS 348 (g/cm <sup>3</sup> )	7.80
Average composition of SS 348 (w/o)	
Fe	69.03
Cr	18.28
Ni	10.95
Mn	1.74
Moderator material	H <sub>2</sub> O
UO <sub>2</sub> linear expansion coefficient (10 <sup>-5</sup> °C <sup>-1</sup> )	0.794
SS linear expansion coefficient (10 <sup>-5</sup> °C <sup>-1</sup> )	1.777
Density of H <sub>2</sub> O at 268°C and 136 atm (g/cm <sup>3</sup> )	0.7820

and burn-up. Selected fuel rods partly from the asymptotic spectrum of the interior region of the fuel boxes and partly from the perturbed spectrum near water gaps and control rods were cut into pieces, and between one and six pellet-size samples from each rod were taken out for analysis. The fuel rods irradiated in the asymptotic spectrum were most of them taken from the corners of the central subassembly, i. e. far from both the box edges and the water hole at the centre of the box.

The analysed samples fall into 3 groups, called phases I, II, and III. Phase I consists of the samples collected after the shutdown of core I. 56 rods from 14 different boxes were removed and a total of 191 samples were prepared, spanning the burn-up range from 1,300 to 18,000 MWD/TU. Two of the irradiated core I elements remained in their places during the second fuel cycle; the rest of the core II loading was identical to the fresh core I fuel. After the final shutdown of core II one of the two elements was destructed to form the 28 phase II samples from 7 different fuel rods. These samples had burn-up values from 10,000 until 31,000 MWD/TU. The last fuel element was kept outside the core during the third cycle and inserted again for further irradiation in core IV. From this element the phase III samples were cut; the 32 phase III samples from 8 fuel rods had burn-up values from 16,000 to 46,000 MWD/TU. But as the highest burn-up samples are those from the rods near water gaps, the asymptotic spectrum measurements used for comparison with pin cell calculations go no further than 40,000 MWD/TU.

In fig. 5.2.b cores I, II, and III with the position of the phase II and III elements are sketched. As the fuel loading of core IV is different from that of cores I and II, the phase III element in its last cycle had other surroundings, but this was estimated to give a production of  $\text{Pu}^{239}$  in the asymptotic rods lowered by only 1/2 - 1 per cent<sup>(22)</sup>.

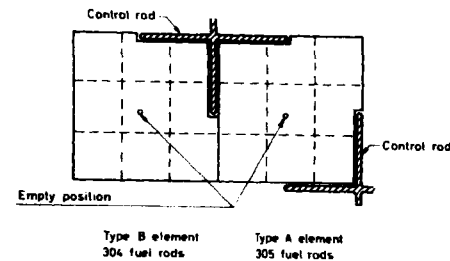


Fig. 5.1.a. Yankee fuel element cross section.

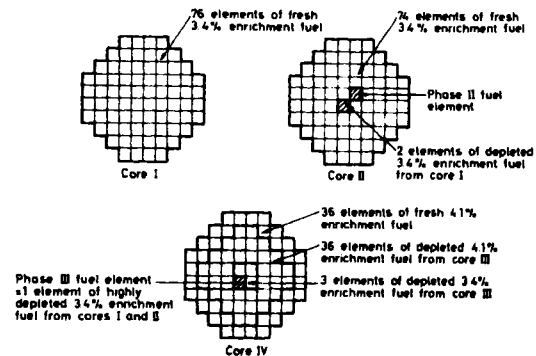


Fig. 5.1.b. Yankee cores I, II, and IV.

5. 2. Unit Cell Burn-up Calculations

In table 5. 2. a the data used for the unit cell burn-up calculation are shown. The pellet-to-clad gap in the fuel rod was homogenized with the  $UO_2$  in contrast to the calculations in ref. 29 where the gap was homogenized with the clad. It seems to be more physically correct to expand the fuel over the entire volume of the fuel tube. The isotope  $U^{234}$  is not included in the burn-up code, so the fuel content of  $U^{234}$  was simply omitted in the calculations. From the components of the cladding SS type 348 the iron, chromium, nickel, and manganese were accounted for individually, and the rest, impurities constituting about one weight per cent of the material, were replaced by iron.

The burn-up calculations were performed by means of the program CEB<sup>29)</sup> with the fission product treatment of the routine FIPO<sup>31)</sup>. Three spatial regions were used for the fuel, clad, and moderator respectively. Initially two time steps of 4 and 12 days are taken to account for the Xe and Sm build-up; then three time steps of 30 days and the number of 60-day steps necessary to reach a burn-up of 45, 600 MWD/TU are applied. This procedure was shown to be adequate in the work of K. E. Lindström Jensen<sup>29)</sup> and was also found to be satisfactory in the calculations on the Dresden I reactor<sup>10)</sup>.

10-group cross sections were supplied from the CRS code, condensed from the 76 groups with the spectrum calculated by the one-dimensional collision probability theory routine GEPUR. In the CRS flux calculation the same three spatial regions as in CEB were applied. The cross sections were regenerated once, at 4200 MWD/TU, to account for the influence on the fine group flux spectrum from Xe, Sm, and the initial Pu build-up. As no data exist on the SIGMA MASTER TAPE for  $Pu^{242}$  a 10-group cross section set for this isotope generated by LASER<sup>16)</sup> was inserted.

Three such burn-up calculations were performed, one where neither the correction to  $U^{238}$  resonance cross sections nor the H removal resonance correction was used, one with only the  $U^{238}$  correction, and one with both corrections. The removal correction is a theoretically based modification of the outscattering cross section in the resonance groups, whereas the  $U^{238}$  is a simple reduction of the resonance integral, introduced because of observed erroneous Pu production results.

Table 5. 2. a

Yankee core I unit cell description (hot, full power)

		Outer region radius (cm)
Fuel ( $UO_2$ )		0.3802
Clad (SS 348)		0.4338
Moderator ( $H_2O$ )		0.6073
		Temperature ( $^{\circ}C$ )
Fuel		578
Clad		280
Moderator		268
		Number density ( $10^{24}$ atoms/cm <sup>3</sup> )
Fuel	$U^{235}$	$7.5089 \times 10^{-4}$
	$U^{236}$	$4.3094 \times 10^{-6}$
	$U^{238}$	$2.1051 \times 10^{-2}$
	O	$4.3621 \times 10^{-2}$
Clad	Fe	$5.7271 \times 10^{-2}$
	Cr	$1.6286 \times 10^{-2}$
	Ni	$8.6422 \times 10^{-3}$
	Mn	$1.4675 \times 10^{-3}$
Mod.	H	$5.2386 \times 10^{-2}$
	O	$2.6193 \times 10^{-2}$
Power density (W/cm)		73.35
Fuel mass density (g U/cm)		3.912
Buckling (cm <sup>-2</sup> )		0.0007

5. 3. Multiplication Factors

The calculated beginning-of-life  $k_{eff}$  is listed in table 5. 3. a for the three types of cross sections together with the measured values taken from ref. 43. For the hot, clean, full-power condition both the CRS values and the CEB values are given, but for the state with equilibrium Xe and Sm concentrations only the CEB values exist.

The CRS-calculated multiplication factors as calculated in the 76 groups of the MASTER TAPE should be the best possible bid of the data system. The 10-group CEB calculations agree with CRS as to the  $k_{\infty}$  values; in the case of  $k_{eff}$  however, a difference of as much as half a per cent is found. This has two reasons: In CRS an incorrect homogenization of the diffusion constant (see also chapter 6), and in CEB an incorrect condensation of the diffusion constant (because the diffusion constant in CEB is made from the 10-group cross sections). Both inaccuracies influence only the buckling term; because of the small dimensions of the Yankee reactor and the correspondingly great buckling the effect is rather significant here. The CRS and the CEB flux and eigenvalue calculations are virtually identical, apart from the number of groups.

The CRS values for the clean condition fall near the lower limit of experimental uncertainty in the case of no corrections and near the upper limit in the case where both corrections are applied. The value with only the  $U^{238}$  correction is higher. The "true" value, however, must lie above the measurement; because the unit cell calculation includes nothing of the irrelevant absorption which is present in the reactor - spacers, control rod followers, and so on, and the  $k_{eff}$  including both corrections is therefore judged to be the best one.

The CEB-calculated values for the equilibrium Xe and Sm condition are situated around the measured value in a manner quite similar to the clean case. This indicates that the contributions from the Xe and Sm are calculated correctly.

Fig. 5.3, a shows the calculated eigenvalue as a function of burn-up with no corrections, with the  $U^{238}$  correction alone, and with both corrections applied. The three curves meet at high burn-up, where the extra  $Pu^{239}$  in the case of no corrections compensates for the high parasitic absorption cross section of  $U^{238}$ .

The measured beginning-of-life multiplication factors and the end-of-life average exposure of core I, obtained from ref. 41, are included for comparison. The curve for no corrections at the first glance seems to fit the measurements best, but considering that a correct overall treatment for the whole core would lower the curves, the agreement is quite as good for the one with both the  $U^{238}$  and the H correction.

Table 5.3.a

Measured eigenvalues for the Yankee reactor compared with unit cell calculations

Hot, clean, full power:	$k_{\infty}$	$\rho$	$k_{eff}$
Measured		$0.0985 \pm 0.0073$	$1.1035 \pm 0.0081^*$
CRS, 76 groups } no corrections	1.1393		1.0963
CEB, 10 groups }	1.1396		1.1007
CRS, 76 groups } $U^{238}$	1.1605		1.1166
CEB, 10 groups } correction	1.1608		1.1211
CRS, 76 groups } $U^{238}$ and	1.1544		1.1106
CEB, 10 groups } H corrections	1.1547		1.1157
<u>Hot, full power, equilibrium Xe and Sm:</u>			
Measured		$0.0693 \pm 0.008$	$1.0718 \pm 0.0090^*$
CEB, 10 groups, no corrections	1.1062		1.0685
CEB, 10 groups, $U^{238}$ correction	1.1266		1.0881
CEB, 10 groups, $U^{238}$ and H corrections	1.1207		1.0824

\*The measured  $k_{eff}$  is obtained as  $\exp(\rho)$ .

#### 5.4. Isotopic Concentrations

In figs. 5.4. b through 5.4. h the calculated isotopic concentrations are compared with the measurements of phases I, II, and III. The measured points are drawn as a function of total accumulated fissions per initial atom of  $U^{238}$  to avoid an eventual systematic error from an incorrect value of the energy released per fission. The connection between the burn-up and the total accumulated fissions is shown in fig. 5.4. a; it is seen that the number of fissions per initial  $U^{238}$  atom is to a first-order approximation  $10^{-3}$  times the burn-up value in GWD/TU. All measurements were taken from ref. 42.

In fig. 5.4. a the experimentally determined points are compared with the CEB calculations. The curves from the three different calculations

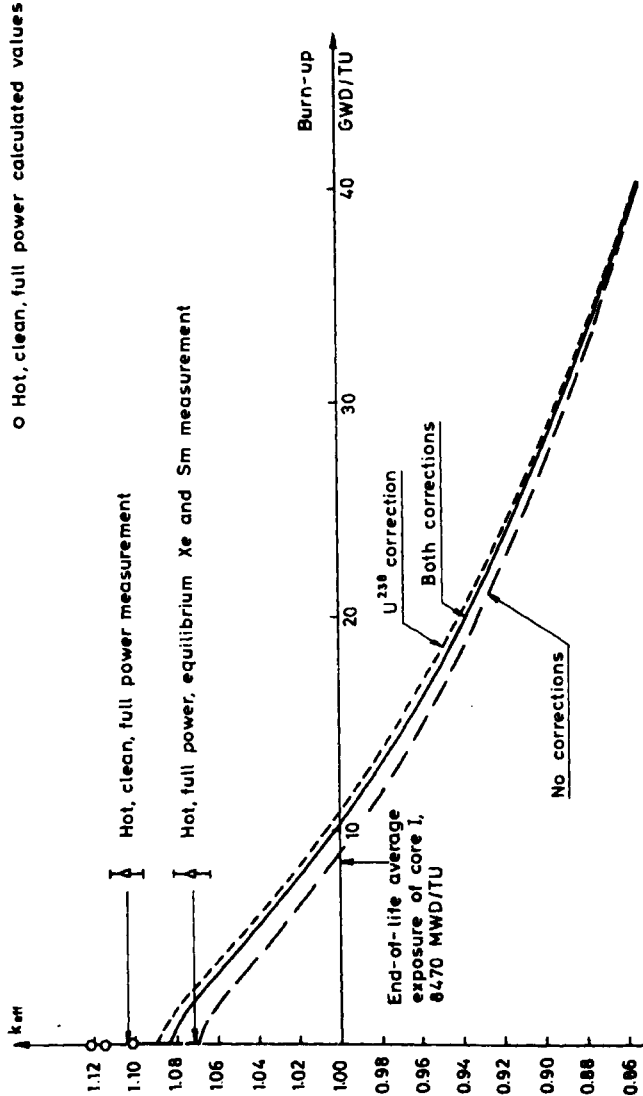


Fig. 5.3.a.  $k_{eff}$  versus burn-up for Yankee unit cell. CEB calculations, hot, full power condition.

cannot be distinguished. Apparently no disagreement is found between the built-in fission energies of CEB and those used in ref. 42.

Figs. 5.4. b - 5.4. d show the destruction or build-up of the uranium isotopes <sup>235</sup>, <sup>236</sup>, and <sup>238</sup>. In the case of U<sup>235</sup> the calculation with neither U<sup>238</sup> nor H removal correction is slightly higher than the one with both corrections; the reason for this is the excessive Pu production in the calculations with uncorrected U<sup>238</sup> cross sections. The corrections seem to give a better agreement with the experimental points. The calculated curve for U<sup>236</sup>, fig. 5.4. c, lies far above the measured values; the reason for this is a too low destruction rate because all thermal cross sections for U<sup>236</sup> are zero in the UKNDL and therefore on the SIGMA MASTER TAPE too. The three calculations give almost identical results for this isotope. In fig. 5.4. d all the three calculated curves for U<sup>238</sup> are drawn; it seems that the one with both corrections is in best agreement with the measurements - at least the uncorrected curve lies a bit too low.

The corresponding curves for the plutonium isotopes 239-242 are given in figs. 5.4. e - 5.4. h. The three different curves can only be distinguished for Pu<sup>239</sup>, so for the rest of the isotopes only one curve is drawn. For the case of Pu<sup>239</sup> shown in fig. 5.4. e the curve with the corrected cross sections is quite acceptable in comparison with the experiments, but perhaps the Pu concentration at high burn-up is a bit too low, indicating either that the reduction of the U<sup>238</sup> cross section is too large or that the absorption cross section of Pu<sup>239</sup> is too high. If the latter is the case, a correspondingly high concentration of Pu<sup>240</sup> should be found in fig. 5.4. f (provided that the Pu<sup>239</sup> a value is correct). In fact the calculation for Pu<sup>240</sup> lies slightly above the measured values, but this again might as well be explained by a too low absorption. A too low Pu<sup>240</sup> absorption is very likely as no Doppler broadening of the resonances is included for this isotope, and at least for the resonance at 1 eV the Doppler broadening is suspected to be important. The calculated Pu<sup>241</sup> concentration in fig. 5.4. g is in good agreement with the experiments and the calculation for Pu<sup>242</sup> in fig. 5.4. h lies slightly higher than the measured points.

As a conclusion drawn from the Yankee calculations the two optional corrections, to the U<sup>238</sup> resonance cross sections and to the removals of H in the resonance groups, seem to improve the agreement with experiment, but possibly the resonance cross sections of U<sup>238</sup> are slightly over-corrected. The calculated isotopic compositions are generally in acceptable agreement with the measurements, although some suspicion is left regarding the data of the Pu isotopes. The uranium isotopic composition is calculated quite satisfactorily, apart from U<sup>236</sup> because of its lack of thermal cross sections.



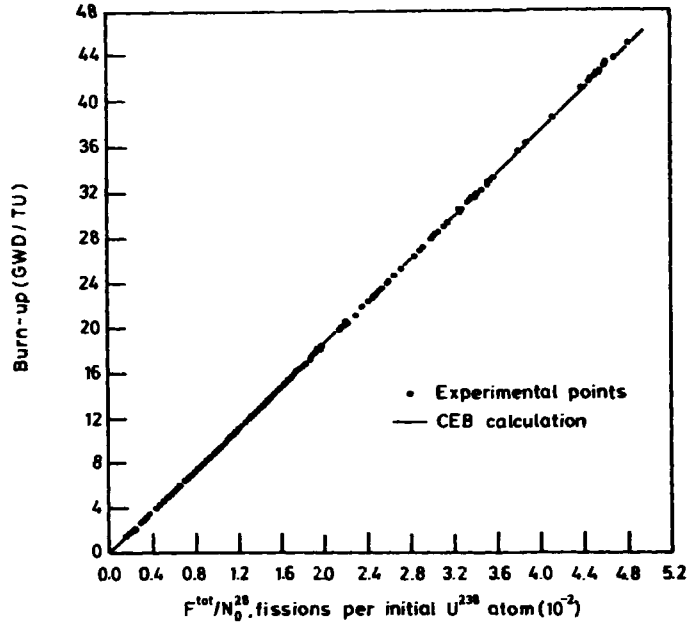


Fig. 5.4. a. Fuel burn-up versus total accumulated fissions.

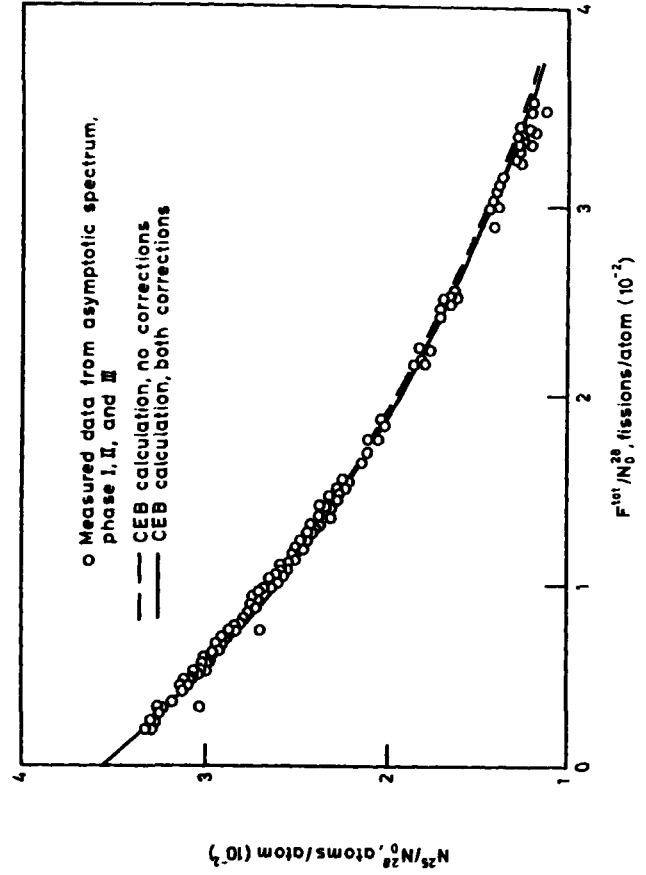


Fig. 5.4. b.  $U^{235}$  concentration versus accumulated fissions.

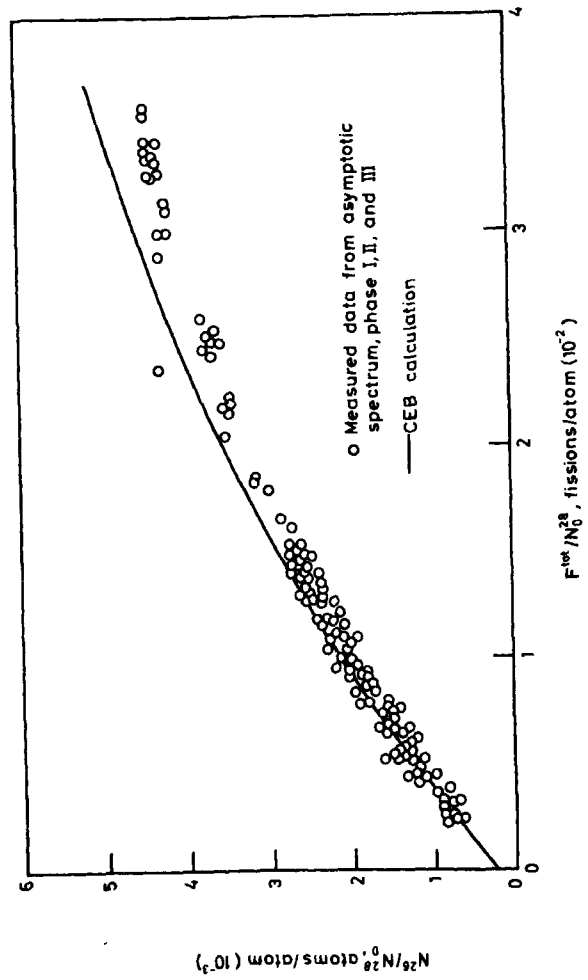


Fig. 5.4.c.  $U^{236}$  concentration versus accumulated fissions.

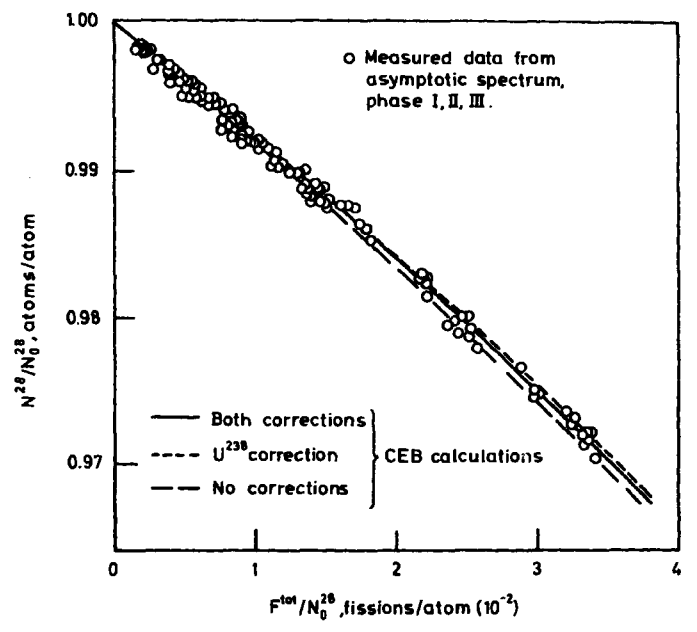


Fig. 5.4.d.  $U^{238}$  concentration versus accumulated fissions.

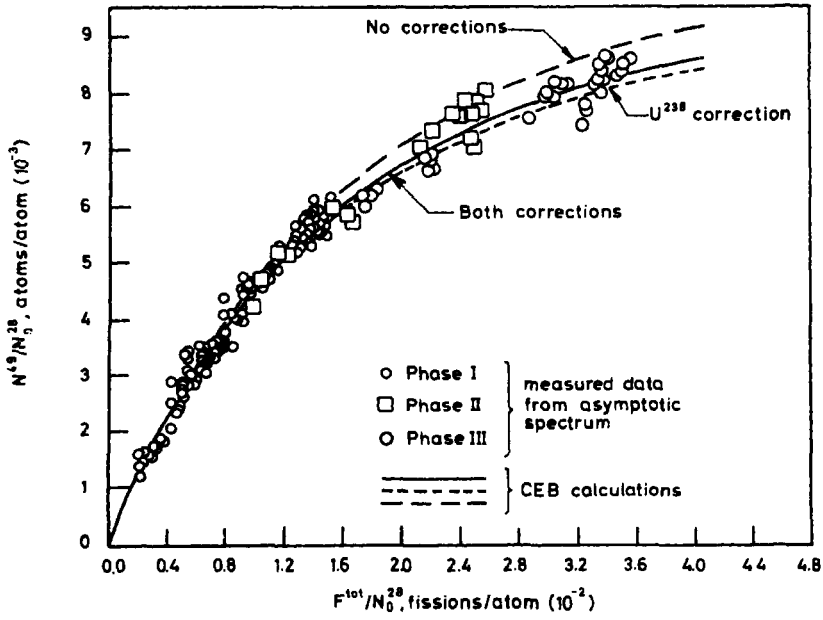


Fig. 5.4.e.  $Pu^{239}$  concentration versus accumulated fissions.

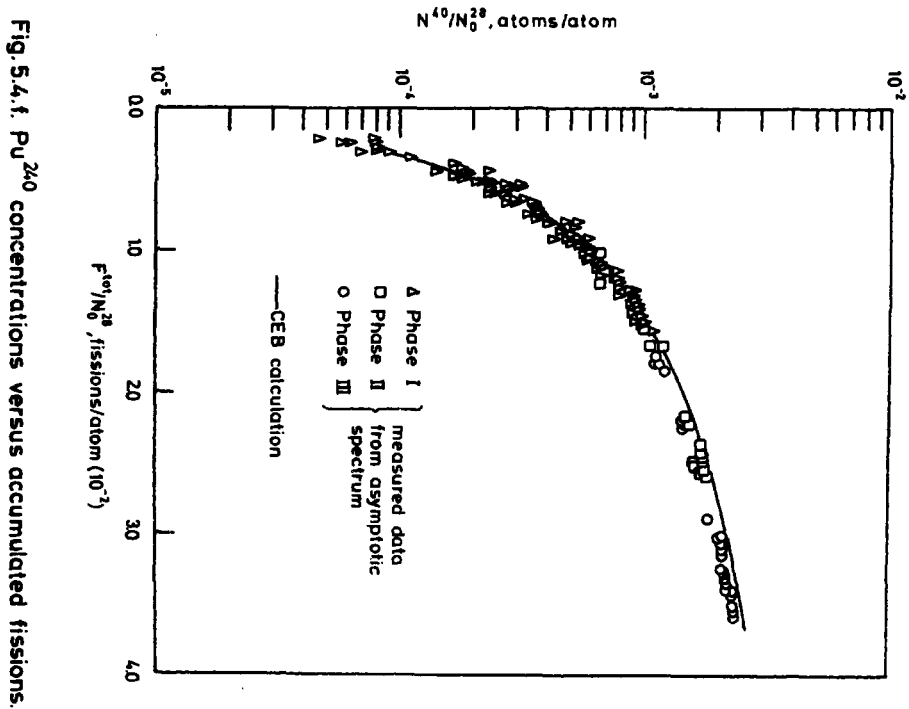


Fig. 5.4.f.  $Pu^{240}$  concentrations versus accumulated fissions.

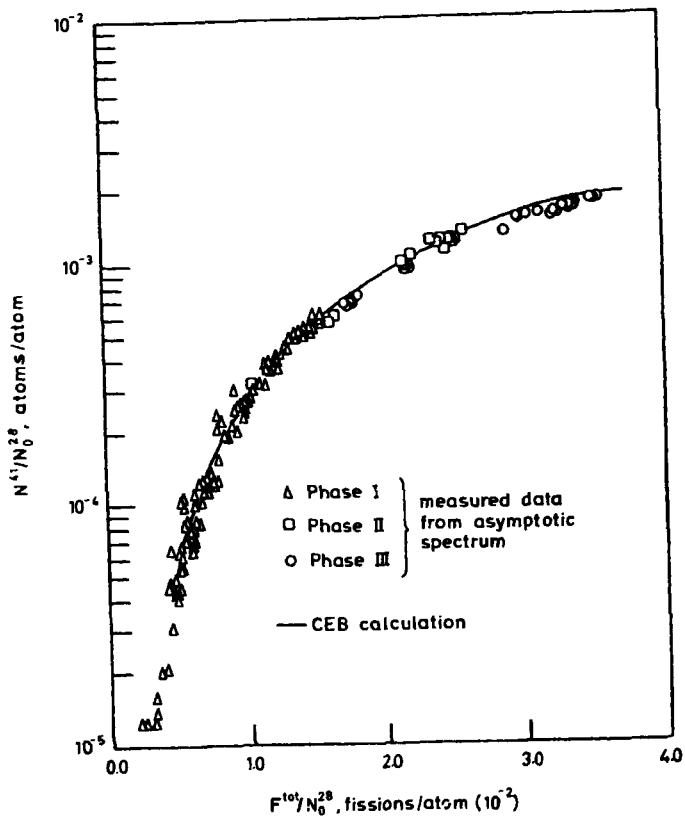


Fig. 5.4.g.  $\text{Pu}^{241}$  concentration versus accumulated fissions.

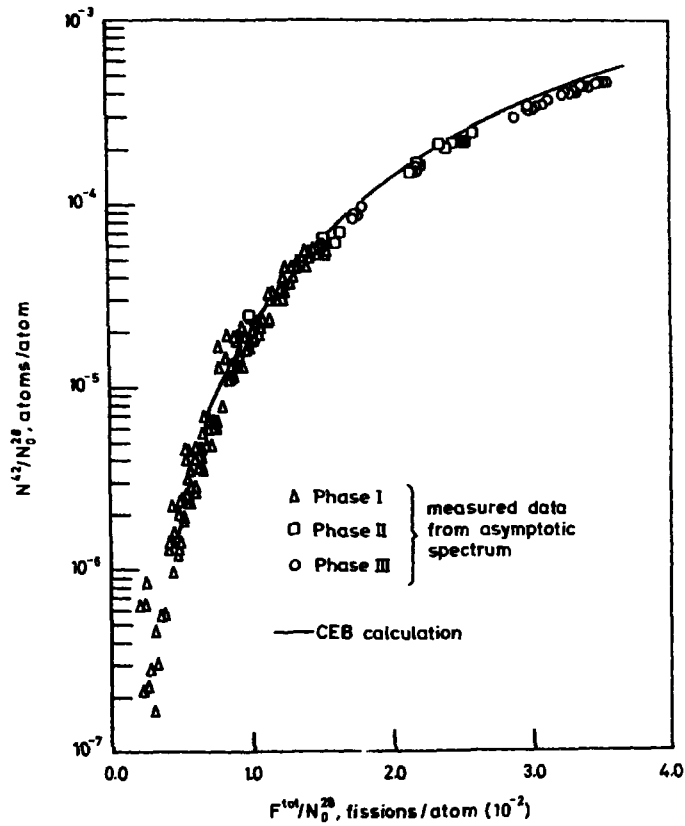


Fig. 5.4.h.  $\text{Pu}^{242}$  concentrations versus accumulated fissions.

## 6. UNIT CELL CRITICALITY CALCULATIONS

An essential feature of any nuclear data system is its reliability in predicting the effective multiplication factor of a given reactor configuration, the more so as the  $k_{\text{eff}}$  calculation is the one most frequently performed in reactor core studies. Besides a very great number of critical experiments on relevant lattices have been carried out and are available in the literature, so it seems very natural to include lattice criticality calculations in the testing of a cross section generating program. By selecting lattices of varying characteristics one is able to evaluate systematic errors which might exist in the basic data or in the data handling.

For the present calculations a number of regular critical lattices were chosen for which measured bucklings were reported. For such lattices the test calculation can be performed in a very simple way in the CRS code itself; a unit cell calculation with the measured overall buckling should give a  $k_{\text{eff}}$  of unity, supposing of course that the buckling value is correct. As most critical experiments have rather small dimensions, the leakage is important and uncertainties in the measured bucklings will greatly affect the calculated eigenvalues. Therefore the resulting  $k_{\text{eff}}$  values must be expected to lie somewhat scattered, but the mean value should be one unless the experiments are biased from systematic errors.

The eigenvalue calculation is done in cylinder geometry by means of the one-dimensional collision probability theory routine of CRS. Three regions are applied, one in the fuel, one in the clad, and one in the moderator, and the energy group structure is the normal 76-group structure of the MASTER TAPE. The two corrections, the resonance depletion correction of the removal cross sections and the reduction of the  $U^{238}$  resonance integral, are used in accordance with the conclusions of chapter 5 of this report. This calculational procedure is the same as the one normally used when spectrum calculations are performed for cross section condensation purposes.

### 6.1. Description of Critical Lattices

In ref. 44 the data are given for 116 well-defined uniform lattices, collected for calculations testing the Westinghouse cell program LEOPARD. The first 55 of these experiments which are fuelled with  $UO_2$ , were considered for the present test calculations, the rest are U metal lattices. As calculations on light-water lattices were found to be the most relevant at the moment, 15 of the experiments were excluded, because they are

moderated by  $H_2O/D_2O$  mixtures. Also the last five experiments were excluded, as large experimental buckling uncertainties are reported for these cases<sup>44</sup>). The data for the remaining 35 test cases are shown in table 6.1. a, where the experiments are identified by the numbers applied in ref. 44.

The equivalent cylinder cells for the lattices span a wide range of the cell parameters which are varied. Enrichment values are found from 1.328 to 4.069 atom per cent  $U^{235}$ , pellet diameters from 0.7544 to 1.5265 cm, equivalent cell radii from 0.5804 to 1.3435 cm, and moderator boron contents from 0 to 3,440 ppm. The measured critical bucklings vary between 17.2 and 95.68  $m^{-2}$ . Stainless-steel clad is used for 25 of the experiments; the remaining 10 experiments have aluminium clad. The aluminium clad with its low absorption cross section behaves almost as zircaloy as regards the neutronics calculations.

The experiments were all performed at room temperature, in the calculations taken as 300 K. The water density used is 1  $g/cm^3$ . The aluminium clad is regarded as pure Al with a density of 2.71  $g/cm^3$ . The SS 304 of the stainless-steel-clad rods contains, according to the AISI specifications, 18-20% Cr, 8-12% Ni, and max. 2% Mn. For the present calculations the composition 19% Cr and 10% Ni was used, and as no information of the Mn content was obtainable, the content 1.74% reported for the Yankee reactor<sup>40</sup>) was taken as a typical value. Because of the great absorption of Mn, this value is important for the calculations. The density of the stainless steel is 7.9  $g/cm^3$ .

Two of the experiments, Nos. 37 and 50, have been used by Slaggie as ENDF/B benchmark tests<sup>38</sup>).

Table 6.1.a.  
Data for critical lattices

Case Number	Enrichment (at. %)	UO <sub>2</sub> density (g/cm <sup>3</sup> )	Pellet diameter (cm)	Clad material	Clad outer diameter (cm)	Clad thickness (cm)	Lattice pitch (cm)	Moderator boron content (ppm)	Measured critical buckling (m <sup>-2</sup> )
1	1.328	7.53	1.5265	Al	1.6916	0.0711	2.205*	0	28.37
2	-	-	-	-	-	-	2.359*	-	30.17
3	-	-	-	-	-	-	2.512*	-	29.06
4	-	7.52	0.9855	-	1.1506	-	1.558*	-	25.28
5	-	-	-	-	-	-	1.652*	-	25.21
6	-	10.53	0.9728	-	-	-	1.558*	-	32.59
7	-	-	-	-	-	-	1.652*	-	35.47
8	-	-	-	-	-	-	1.806*	-	34.22
9	2.734	10.18	0.7620	SS 304	0.8594	0.0408	1.0287	-	40.75
10	-	-	-	-	-	-	1.1049	-	53.23
11	-	-	-	-	-	-	1.1938	-	63.28
12	-	-	-	-	-	-	1.4554	-	65.64
13	-	-	-	-	-	-	1.5621	-	60.07
14	-	-	-	-	-	-	1.6891	-	52.92
15	-	-	-	-	-	-	1.0617	-	47.5
16	-	-	-	-	-	-	1.2522	-	68.8
17	3.745	10.37	0.7544	-	0.8600	0.0406	1.0617	-	68.3
18	-	-	-	-	-	-	1.2522	-	95.1
19	-	-	-	-	-	-	-	-	95.68
20	-	-	-	-	-	-	-	482	74.64
21	-	-	-	-	-	-	-	718	63.66
22	-	-	-	-	-	-	-	1278	40.99
23	-	-	-	-	-	-	-	1350	38.39
24	-	-	-	-	-	-	-	1495	33.38
25	4.069	9.46	1.1278	-	1.2090	-	1.5113	0	88.0
26	-	-	-	-	-	-	-	3440	17.2
34	-	-	-	-	-	-	1.450	0	79.0
37	2.490	10.24	1.0297	Al	1.2060	0.0813	1.5113	-	70.10
42	3.037	9.28	1.1288	SS 304	1.2701	0.0716	1.555	-	60.75
43	-	-	-	-	-	-	2.198	-	68.61
44	4.069	9.45	-	-	-	-	1.555	-	69.25
45	-	-	-	-	-	-	1.684	-	65.52
46	-	-	-	-	-	-	2.198	-	92.84
47	-	-	-	-	-	-	2.381	-	91.79
50	2.490	10.24	1.0297	Al	1.2060	0.0813	1.5113	1585	20.2

\* Triangular lattices; all others are square

## 6.2. Calculated Multiplication Factors

In GEPUR, the collision probability theory flux calculation routine of CRS, the  $k_{\text{eff}}$  is calculated after the flux calculation by adding the term  $DB^2$  to the absorption cross section in all regions and dividing the total neutron production by the total absorption ( $D$  = diffusion constant,  $B$  = buckling). The buckling specified has no influence on the calculated flux. For the present lattice calculations where the buckling values are unusually high, this procedure yields inaccurate  $k_{\text{eff}}$  results, because in fact it involves a wrong homogenization method for the diffusion constant; especially the  $k_{\text{eff}}$  values obtained for the Al clad lattices are wrong. Therefore the  $k_{\text{eff}}$  given in the CRS code was ignored, and another  $k_{\text{eff}}$  obtained from the homogenized cell constants is reported here.

For the calculation the equivalent cylinder cell dimensions and the number densities were calculated from the data given in table 6.1.a. Where a pellet-to-clad gap exists, it was homogenized with the clad, as this was expected to do less harm than if the fuel was expanded to fill out the clad tubes; for zero power experiments as those investigated here, the fuel pellets presumably keep their initial dimensions in contrast to the case of power reactors.

The calculated multiplication factors,  $k_{\text{inf}}$  and  $k_{\text{eff}}$  are given in tables 6.2.a to 6.2.f for the 35 cases of table 6.1.a. The experiments were divided into groups of related lattices, to give the possibility of investigating differences between the individual series of experiments.

In fig. 6.2.b the calculated values of  $k_{\text{eff}}$  are shown as a function of the measured buckling value. The mean calculated  $k_{\text{eff}}$  is 0.9941. The different experiment series were assigned the symbols given in fig. 6.2.a; the open symbols refer to the two series of Al clad lattices and the rest to those with SS clad. As was to be expected the points lie somewhat more dispersed at the higher buckling values, otherwise no trends are deduced from the plot versus buckling.

To investigate if systematic data errors affect the calculated multiplication factors, the data were plotted as a function of different important cell parameters. In fig. 6.2.c the calculated points are shown versus enrichment and in fig. 6.2.d versus the fuel region diameter; neither of the two plots shows any trend of the calculation. But in fig. 5.2.e the calculated  $k_{\text{eff}}$  values are plotted against the cell ratio of H to U<sup>235</sup> atoms, and here the calculated  $k_{\text{eff}}$  shows a tendency to decrease with increasing moderating ratio. For the lattices with a H to U<sup>235</sup> atom ratio below 200

the mean value seems to be close to one, whereas all points of higher moderating ratio fall below the line of unity. The same trend is found for the individual measurement series. As realistic light-water reactor lattices are well under-moderated, their multiplication factors according to this should be predicted fairly accurately. The Yankee reactor unit cell dealt with in chapter 5 of this report has a H to  $U^{235}$  ratio of 87.18.

In fig. 6.2. f the effective multiplication factors are shown as a function of boron content in the moderator for the three experiment series where the moderator boron poisoning was varied. A slight tendency of  $k_{eff}$  to decrease with increasing boron content is found, but the two-point series in which the greatest boron concentration is found shows the opposite trend, so no definite conclusion can be drawn from the present material.

The only certain indication of systematic errors is found in the dependence of  $k_{eff}$  upon the moderating ratio. It is difficult to say if the reason is for instance an error in the resonance data or in the thermal scattering data or both. The fact that the triangular lattices Nos. 1-8 have almost constant  $k_{eff}$  values over a wide range of moderating ratios points towards the Dancoff factor, but the explanation might as well be that the H removal correction simply over-corrects at the high moderating ratios.

○	Data from table	6.2.a
●	" " "	6.2.b
▲	" " "	6.2.c
x	" " "	6.2.d
■	" " "	6.2.e
△	" " "	6.2.f

Fig.6.2. a. Key to figs. 6.2. b through 6.2.f.

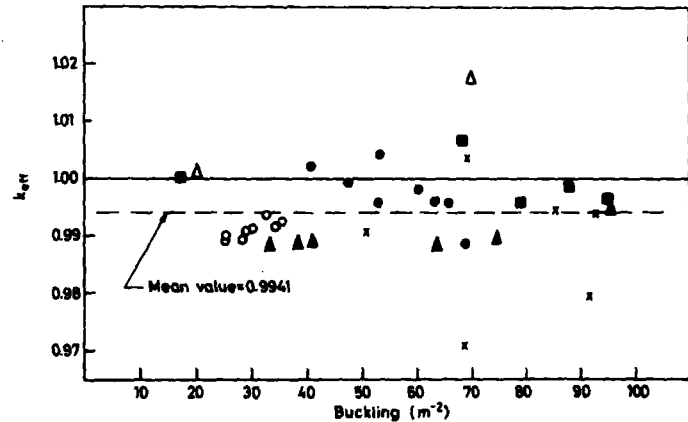


Fig.6.2.b. Calculated  $k_{eff}$  versus experimental buckling.

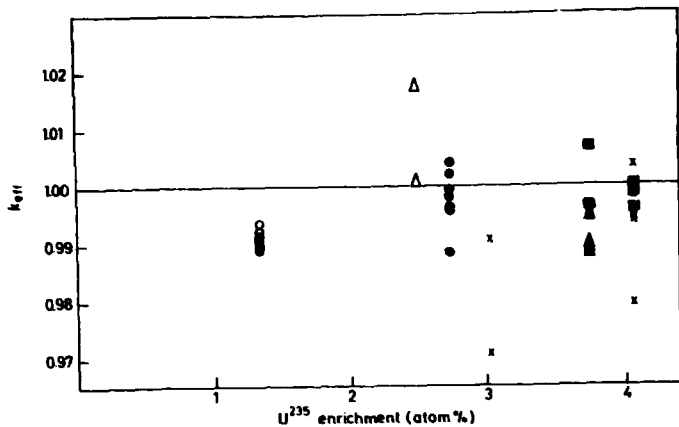


Fig. 6.2.c Calculated  $k_{eff}$  versus enrichment

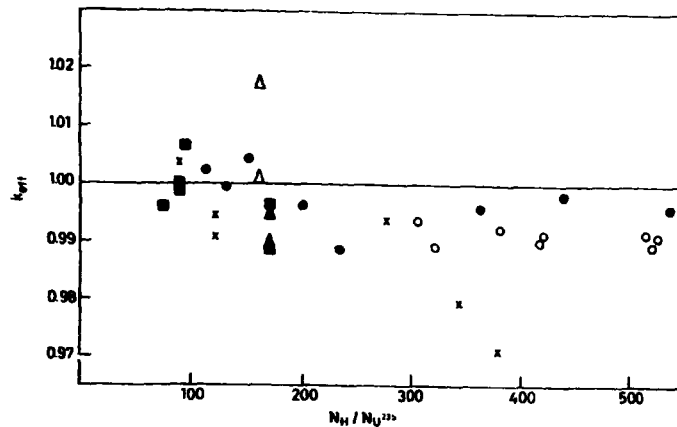


Fig 5.2.e. Calculated  $k_{eff}$  versus H to  $U^{235}$  atom ratio.

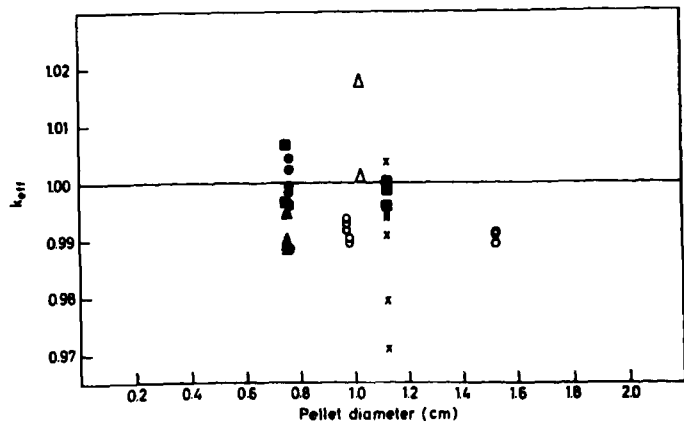


Fig. 6.2.d Calculated  $k_{eff}$  versus rod size

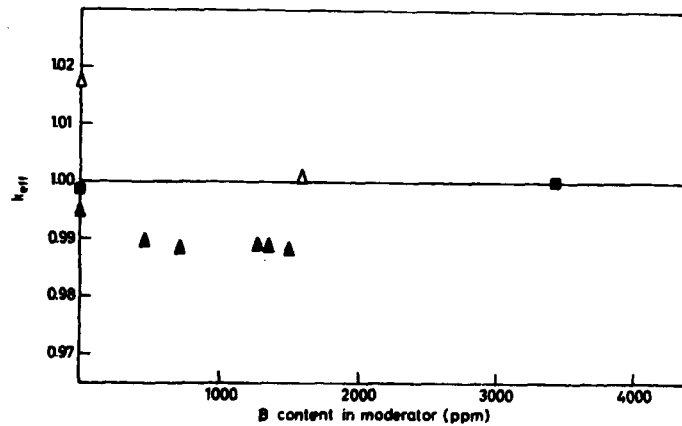


Fig. 6.2.f. Calculated  $k_{eff}$  versus moderator boron content.



Table 6.2.a.

Triangular lattices, Al clad, no boron

Case No.	1	2	3	4	5	6	7	8
$k_{inf}$	1.1440	1.1440	1.1298	1.1248	1.1156	1.1369	1.1415	1.1289
$k_{eff}$	0.9892	0.9912	0.9908	0.9899	0.9891	0.9936	0.9923	0.9914

Table 6.2.b

SS clad, square lattices, pitch varied

Case No.	9	10	11	12	13	14	15	16
$k_{inf}$	1.1667	1.2049	1.2283	1.2259	1.2080	1.1797	1.1859	1.2352
$k_{eff}$	1.0021	1.0042	0.9961	0.9958	0.9981	0.9957	0.9993	0.9886

Table 6.2.c

SS clad, square lattices, moderator boron content varied

Case No.	19	20	21	22	23	24
$k_{inf}$	1.3365	1.2542	1.2133	1.1335	1.1240	1.1057
$k_{eff}$	0.9946	0.9896	0.9883	0.9889	0.9887	0.9882

Table 6.2.d

SS clad, square lattices, pitch varied (two enrichments)

Case No.	42	43	44	45	46	47
$k_{inf}$	1.1968	1.2108	1.2821	1.3178	1.3195	1.2945
$k_{eff}$	0.9906	0.9708	1.0035	0.9943	0.9937	0.9793

Table 6.2.e.

Miscellaneous SS clad square lattices

Case No.	17	18	25	26	34
$k_{inf}$	1.2742	1.3365	1.3446	1.0676	1.3161
$k_{eff}$	1.0065	0.9962	0.9985	1.0001	0.9957

Table 6.2.f

Al clad, square lattices, moderator boron content varied

Case No.	37	50
$k_{inf}$	1.3255	1.0874
$k_{eff}$	1.0174	1.0009

## 7. CONCLUSION

A data-generating system which utilizes physical basic data was constructed, and it seems to work rather satisfactorily for light-water reactor calculations. Although the library used, UKNDL version 1968, has been updated, it seems unnecessary to change to the new version, the more so, as for practical calculation purposes experience from a great number of calculations is by far the most important for the confidence one may have in the predictions from a code complex.

As regards the data for the plutonium isotopes the situation is different. Both the plutonium spheres of chapter 4 and to some extent the burn-up calculations of chapter 5 indicate errors in the plutonium cross sections, so it seems that the basic library, the SIGMA MASTER TAPE, should be updated if systems for which these are of great influence are to be dealt with, for instance fast breeder reactors or thermal reactors containing reprocessed fuel. Perhaps a more detailed resonance treatment for the plutonium isotopes will also prove desirable.

## ACKNOWLEDGEMENTS

The author wishes to thank all members of the Reactor Physics Department at Risø for their assistance. Especially the continuous help of H. Neltrup is gratefully acknowledged.

REFERENCES

- 1) K. Parker, The Aldermaston Nuclear Data Library as at May 1963. AWRE 0-70/63 (1963) 64 pp.
- 2) D.S. Norton, The UKAEA Nuclear Data Library, February 1968. AEEW - M 824 (1968) 23 pp.
- 3) A. M. Hvidtfeldt Larsen, SIGMA MASTER TAPE, a Multigroup Cross Section Library. Risø Report No. 262 (1972) 50 pp.
- 4) A. M. Hvidtfeldt Larsen, CRS: A Code to Produce Multigroup Neutron Cross Sections for Reactor Physics Calculations. Risø-M-1568 (1973).
- 5) A. F. Henry, Panel Discussion on Outstanding Problems. In: Numerical Reactor Calculations, Proceedings of a Seminar, Vienna, 17-21 January 1972 (IAEA, Vienna, 1972) 550.
- 6) J. J. Schmidt, General Status of Nuclear Data Requirements. In: Second International Conference on Nuclear Data for Reactors, Conference Proceedings, Helsinki, 15-19 June 1970 (IAEA, Vienna, 1970) 3-15.
- 7) B. H. Patrick and M. G. Sowerby, Report on the Evaluation Working Group Meeting Held 26-28 January 1972 at A. E. R. E., Harwell, U. K. to Discuss the Evaluation of  $U^{235}$ ,  $U^{238}$  and  $Pu^{239}$  Cross-Sections. EANDC-90 "L" (1972) 71 pp.
- 8) Data Formats and Procedures for the ENDF Neutron Cross Section Library. Edited by M. K. Drake. BNL 50274 (1970) 200 pp.
- 9) D. Woll, Card Image Format of the Karlsruhe Evaluated Nuclear Data File KEDAK. KFK 880 (1968) 18 pp.
- 10) A. M. Hvidtfeldt Larsen, H. Larsen, and T. Petersen, Calculations on a Boiling Water Reactor as a Test of the Risø Reactor Code Complex. Risø Report No. 268 (1972) 102 pp.
- 11) H. Neltrup, Benchmark Calculations on Homogeneous Spheres. Risø-M-1526 (1972) 11 pp.
- 12) L. Mortensen and H. Neltrup, Risø, Denmark, Personal Communication, 1972.
- 13) H. Neltrup and P. B. Suhr, Risø, Denmark. Personal Communication, 1972-1973.

- 14) J. Pedersen, A Preliminary Description of the SIGMA Programme. Risø-M-949 (1969) (Internal Report) 29 pp.
- 15) V. J. Bell et al., A User's Guide to GALAXY 3. AEEW-R-379 (1964) 58 pp.
- 16) C. G. Poncelet, LASER - A Depletion Program for Lattice Calculations based on MUFT and Thermos. WCAP-6073 (1966) 104 pp.
- 17) H. C. Honeck, The Calculation of the Thermal Utilization and Disadvantage Factor in Uranium/Water Lattices. Nucl. Sci. Eng. 18 (1964) 49-68.
- 18) J. Mikkelsen, The Neutron Resonance Reactions in Thermal Nuclear Reactors Determined by Semi-Analytic as well as Numerical Methods. Risø Report No. 234 (1970) 167 pp.
- 19) J. Mikkelsen and P. Kirkegaard, A User's Guide to the RESAB Program System for the B 6700 Computer. Risø-M-1477 (1972) 53 pp.
- 20) A. M. Hvidtfeldt Larsen, Resonanstværsnit. Master's Thesis, Danish Atomic Energy Commission, Risø, (in Danish, 1969) 125 pp. Not published.
- 21) H. Neltrup, RESOREX, A Procedure for Calculating Resonance Group Cross-Sections. Risø-M-1437 (1971) 25 pp.
- 22) J. R. Askew, The Calculation of Resonance Captures in a Few-Group Approximation. AEEW-R-489 (1966) 22 pp.
- 23) F. J. Fayers, P. B. Kemshell, and M. J. Terry, An Evaluation of Some Uncertainties in the Comparison between Theory and Experiment for Regular Light-Water Lattices. J. Brit. Nucl. Energy Soc. 6 (1967) 166.
- 24) C. F. Højerup, Om procedure NELKINSCM til beregning af termiske spredningsdata. Risø-M-1379 (in Danish, 1971) (Internal Report) 11 pp.
- 25) C. F. Højerup, Risø, Denmark, unpublished work 1972.
- 26) H. C. Honeck and D. R. Finch, FLANGE II (Version 71-1), A Code to Process Thermal Neutron Data from an ENDF/B Tape. DP-1278 (1971) 121 pp.
- 27) A Compilation of Evaluations of Neutron and Photon Cross Sections Available May 1972. CCDN-NW/14 (1972) 133 pp.
- 28) H. Neltrup, Integral Transport Theory in Various Geometries. Risø-M-1289 (1970) 16 pp.

- 29) K. E. Lindstrøm Jensen, Development and Verification of Nuclear Calculation Methods for Light-Water Reactors. Risø Report No. 235 (1970) 161 pp.
- 30) C. F. Højerup, User's Manual for the Programme CDB 2 as of October 1st, 1972. Risø-M-1546 (Internal Report) (1972) 21 pp.
- 31) L. Mortensen, The Fission Product Treatment in the CEB Unit Cell Burn-up Programme. Risø-M-1356 (1971) 69 pp.
- 32) H. Larsen, Approximate Methods for 3D Overall Calculations on Light Water Reactors. Risø Report No. 270 (1972) 48 pp.
- 33) K. D. Lathrop, DTF 4, A Fortran - IV Program for Solving the Multi-group Transport Equation with Anisotropic Scattering. LA-3373 (1965) 141 pp.
- 34) K. D. Lathrop, User's Guide for the TWOTRAN (x, y) Program. LA-4058 (1968) 23 pp.
- 35) R. Gwin and D. W. Magnuson, Critical Experiments for Reactor Physics Studies. CF-60-4-12 (1960) 64 pp.
- 36) R. Gwin and D. W. Magnuson, The Measurement of Eta and Other Nuclear Properties of  $U^{233}$  and  $U^{235}$  in Critical Aqueous Solutions. Nucl. Sci. Eng. 12 (1962) 364-380.
- 37) F. E. Kruesi, J. O. Erkman, and D. D. Lanning, Critical Mass Studies of Plutonium Solutions. HW-24514 DEL (1952) 85 pp.
- 38) E. L. Slaggie, Thermal Benchmark Calculations for Water-Moderated Uranium- and Plutonium-Fuelled Systems. GULF-RT-10337 (EACRP A 137) (1971) 40 pp.
- 39) A. Staub, D. R. Harris, and Mark Goldsmith, Analyses of a Set of Critical Homogeneous  $U-H_2O$  Spheres. Nucl. Sci. Eng. 34 (1968) 263-274.
- 40) H. W. Graves, R. F. Janz, and C. G. Poncelet, The Nuclear Design of the Yankee Core. YAEC-136 (1961) 88 pp.
- 41) R. J. Nodvik, Evaluation of Mass Spectrometric and Radiochemical Analyses of Yankee Core I Spent Fuel. WCAP-6068 (1968) 181 pp.
- 42) R. J. Nodvik et al., Supplementary Report on Evaluation of Mass Spectrometric and Radiochemical Analyses of Yankee Core I Spent Fuel, Including Isotopes of Elements Thorium Through Curium. WCAP-6086 (1969) 259 pp.

- 43) C. G. Poncelet, Analysis of the Reactivity Characteristics of Yankee Core I. WCAP-6050 (1963) 139 pp.
- 44) L. E. Strawbridge and R. F. Barry, Criticality Calculations for Uniform Water-Moderated Lattices. Nucl. Sci. Eng. 23 (1965) 58-73.

